

IDENTIFICATION AND COMPENSATION OF FRICTION FOR A DUAL STAGE  
POSITIONING SYSTEM

A Thesis

by

SATISH THIMMALAPURA

Submitted to the Office of Graduate Studies of  
Texas A&M University  
in partial fulfillment of the requirements for the degree of

MASTER OF SCIENCE

August 2004

Major Subject: Mechanical Engineering

IDENTIFICATION AND COMPENSATION OF FRICTION FOR A DUAL STAGE  
POSITIONING SYSTEM

A Thesis

by

SATISH THIMMALAPURA

Submitted to Texas A&M University  
in partial fulfillment of the requirements  
for the degree of

MASTER OF SCIENCE

Approved as to style and content by:

---

Reza Langari  
(Co-Chair of Committee)

---

Craig Smith  
(Co-Chair of Committee)

---

Arun Srinivasa  
(Member)

---

Srinivas Vadali  
(Member)

---

Dennis O'Neal  
(Head of Department)

August 2004

Major Subject: Mechanical Engineering

## ABSTRACT

Identification and Compensation of Friction for a Dual Stage Positioning System. (August 2004)

Satish Thimmalapura, B.E., Bangalore University, India

Co-Chairs of Advisory Committee: Dr. Craig Smith  
Dr. Reza Langari

Motion control systems are usually designed to track trajectories and/or regulate about a desired point. Most of the other objectives, like minimizing the tracking time or minimizing the energy expended, are secondary which quantify the above described objectives. The control problem in hard disk drives is tracking and seeking the desired tracks. Recent increase in the storage capacity demands higher accuracy of the read/write head. Dual stage actuators as compared to conventional single actuator increases the accuracy of the read/write head in hard disk drives. A scaled up version of the dual stage actuator is considered as the test bed for this thesis. Friction is present in all electromechanical systems.

This thesis deals with modelling of the dual stage actuator test bed. A linear model predicts the behavior of the fine stage. Friction is significant in the coarse stage. Considerable time has been spent to model the coarse stage as a friction based model. Initially, static friction models were considered to model the friction. Dynamic models, which describe friction better when crossing zero velocity were considered. By analyzing several experimental data it was concluded that the friction was dependent on position and velocity as compared to conventional friction models which are dependent on the direction of motion. Static and Coulomb friction were modelled as functions of velocity and position. This model was able to predict the behavior of the coarse stage satisfactorily for various

initial conditions. A friction compensation scheme based on the modelled friction is used to linearize the system based on feedback linearization techniques.

To my family and friends.

## ACKNOWLEDGMENTS

This thesis would not have been possible without the help and guidance of many people. First and foremost, I would like to express my gratitude to my advisors, Professors Reza Langari and Craig Smith, without whose guidance this thesis would not have been accomplished. I am thankful to Dr. Smith for his invaluable suggestions. I am very thankful to Dr. Langari for advising me through the final stages of the thesis despite all his other commitments and also for his patience.

I wish to thank Professor Arun Srinivasa and Professor Srinivas Vadali for serving on my thesis committee.

I would like to thank all my colleagues at Mechanical Engineering Controls & Robotics Lab, TAMU for their time and constructive suggestions. I would also like to thank Dnyanesh Khot for helping me with setting up the laboratory test bed. Also, Ankush Wattal for all his timely suggestions.

My wholehearted gratitude to my family and friends, for their love, support and encouragement.

## TABLE OF CONTENTS

CHAPTER		Page
I	INTRODUCTION . . . . .	1
II	BACKGROUND . . . . .	3
	A. Hard Disk Drives and Dual Stage Actuators . . . . .	3
	B. Friction Models . . . . .	4
	C. Effect of Friction on Dynamic Systems . . . . .	10
	D. System Identification and Modelling . . . . .	13
III	EXPERIMENTAL SETUP . . . . .	15
IV	MODELLING . . . . .	19
	A. VCM Model (Fine Stage) . . . . .	19
	B. Coarse Stage . . . . .	19
	1. MATLAB Toolbox . . . . .	21
	2. Parametric Modelling . . . . .	21
	3. Coulomb Friction and Stiction Model . . . . .	23
	4. Position Dependent Friction Model . . . . .	28
	5. Model Considering the Drive Train . . . . .	29
	6. Dynamic Model with Memory . . . . .	31
	7. Estimation of the Linear Parameters . . . . .	32
	C. Summary of experiments . . . . .	35
	1. Random Triangular Signal . . . . .	35
	2. Hysteresis/Asymmetry . . . . .	35
	3. Velocity Limit Experiment . . . . .	39
	D. Position and Direction Dependent Models . . . . .	39
	1. Results . . . . .	45
	2. Friction Compensation . . . . .	49
V	CONCLUSIONS AND FUTURE WORK . . . . .	57
	REFERENCES . . . . .	59
	VITA . . . . .	62

## LIST OF FIGURES

FIGURE	Page
1	Hard disk drive assembly (Adapted from [1]) . . . . . 4
2	Static friction models . . . . . 6
3	Interaction between the bristles of two surfaces (Adapted from [2]) . . . . . 8
4	Stress-strain curve (Adapted from [3]) . . . . . 8
5	Dahl model-friction vs position (Adapted from [4]) . . . . . 9
6	Stick slip motion of a mass subjected to the above input . . . . . 11
7	Schematic of the application of dither signal . . . . . 12
8	Model based friction compensation scheme . . . . . 13
9	Dual stage actuator test bed . . . . . 16
10	Block diagram of the dual stage positioning test bed . . . . . 18
11	Comparison of the actual output and the model output for the fine stage . . . . . 20
12	Comparison of the actual output and the model output, at steady state, for the coarse stage considering Coulomb friction . . . . . 23
13	Comparison of the actual output and the model output, input being zero mean, white Gaussian noise, for the coarse stage considering Coulomb friction . . . . . 24
14	Comparison of the actual output and the model output, at steady state, for the coarse stage considering Coulomb friction and stiction . . . . . 25
15	Comparison of the actual output and the model output with zero mean, white Gaussian noise as the input for the coarse stage, considering Coulomb friction and stiction . . . . . 26



FIGURE	Page
16	Drift of the slider in the open loop when starting from the left end (10mm) 27
17	Drift of the slider in the open loop when starting from the right end (205mm) 27
18	Parabolic friction map . . . . . 28
19	Comparison of the actual and model output for a sinusoidal signal considering Coulomb friction to be parabolic . . . . . 29
20	Comparison of the simulation and the actual output for a zero mean sinusoidal input signal considering drive train model . . . . . 31
21	Comparison of the simulation and the actual output for a zero mean, sinusoidal input signal, considering Dahl model . . . . . 33
22	Random triangular input signal . . . . . 36
23	Displacement of the slider with the forcing function . . . . . 37
24	Displacement vs voltage: different cases . . . . . 38
25	Velocity limit experiment . . . . . 40
26	Direction and position dependent stiction model . . . . . 41
27	Comparing the response of the above described model with the actual response . . . . . 43
28	The response of the slider to a constant signal . . . . . 44
29	Stiction profile along the length of the slider . . . . . 46
30	Stiction profile . . . . . 48
31	Comparison of the open loop response of the model and the system, while starting at 10mm . . . . . 50
32	Comparison of the open loop response of the model and the system, while starting at 205mm . . . . . 51
33	Comparison of the open loop response of the model and the system, while starting at 115mm and 250mm . . . . . 52

FIGURE		Page
34	Comparison of the open loop response of the model and the system for a zero mean square wave input . . . . .	53
35	Comparison of the response of the system with and without friction compensation . . . . .	55
36	Comparison of the response of the system with friction compensation and the response of an equivalent linear system . . . . .	56

## LIST OF TABLES

TABLE	Page
I Experimental Data . . . . .	47

## CHAPTER I

### INTRODUCTION

Motion control subsystems are critical components in many electromechanical systems (automobiles, spacecrafts, disk drives, robotics). Typical control objectives are trajectory tracking and/or regulation about a desired point or position. Secondary objectives for the control system might be minimizing the tracking time, optimizing the energy expended for tracking or regulating, etc. In this thesis, a dual stage positioning system is considered to consist of a fine actuator and a coarse actuator. The two actuators work together in trajectory tracking and/or regulating about a desired position. Dual stage actuators have been introduced to improve the servo performance in disk drive control systems. As a result of the dual stage actuator implementation, areal density (tracks per inch) of hard disk drives has been improved. This increases the storage capacity of hard disk drive for the same given area. A dual stage actuator with friction in the coarse stage is considered for this thesis.

Backlash in gears, actuator limits, control signal saturation, exogenous inputs, etc may affect the behavior of electromechanical systems. Mechanical friction has a pronounced effect on the system behavior when controlling systems at low velocities and/or systems which are changing directions. Friction compensation refers to cancelling the effect of friction through some control action.

Friction compensation can be achieved based on the approximate model of friction. A mathematical model of a system is developed based on observations. The model is considered to be useful if it can predict the system behavior. System identification consists of experimentally collecting system response to a particular input, choosing a structure for

---

The journal model is *IEEE Transactions on Automatic Control*.

the system and then determining the parameters of the model based on the structure chosen. Building an accurate model of the system and the friction will allow one to use the control signal aggressively to achieve the performance objectives.

This thesis deals with system identification and friction compensation for a dual stage positioning system. The system under consideration is a test bed in the laboratory which will be used for experimental studies. The objectives of this thesis are:

- 1) Modelling the dual stage actuator system.
  - 1.1) Modelling the fine stage
  - 1.2) Validating the fine stage model
  - 1.3) Modelling friction for the coarse stage actuator.
  - 1.4) Validating the model by comparing simulation and experiment.
- 2) Designing friction compensation for the coarse stage using the developed friction model.

## CHAPTER II

### BACKGROUND

This chapter gives insight into why dual stage positioning systems are being used in hard disk drives. It also delves into the control problem associated with the dual stage positioning system. This chapter also talks about various kinds of friction, the development of friction models over the years and the effect of friction on dynamical systems.

#### A. Hard Disk Drives and Dual Stage Actuators

Magnetic hard disk storage capacity has grown at a tremendous rate in the recent years. The capacity of the hard disk drives (HDDs) has increased from around 2GB in 1996 to around 60GB in 2004. The areal density of the HDDs has been increasing by around 60% every year [5]. With increasing storage capacity, the track density i.e. number of tracks per inch (TPI) and the bit density i.e. number of bits per inch (BPI) is also increasing. With increased TPI and BPI, the position accuracy of the HDD recording head has to be increased to read/write data on to the HDD.

The hard disk drive assembly is shown in Figure 1. Several disks are mounted on the spindle motor. There is a recording head corresponding to each disk surface. The recording head at the tip of the carriage extending from the voice coil motor (VCM) reads/writes data on to the disk. The recording head floats on the air bearing between the head and the disk. The flexible printed circuit connects the wires from the head to motor control unit.

The VCM with its limited bandwidth is not able to achieve increased levels of accuracy. In order to achieve higher accuracies a second actuator with higher bandwidth is used in conjunction with the VCM. The second actuator is mounted at the tip of the carriage. The recording head is to be mounted on the second actuator. Piezoelectric, electromagnetic and electrostatic actuators can be used as secondary actuator. In the dual stage system,

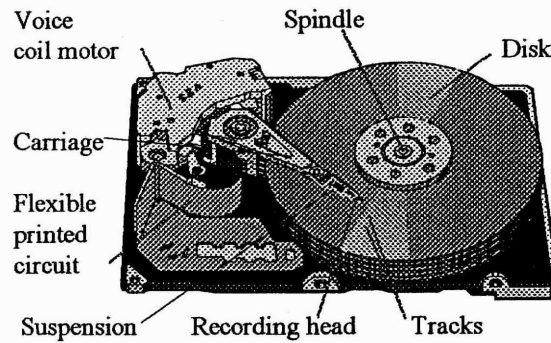


Fig. 1. Hard disk drive assembly (Adapted from [1])

VCM is referred to as the coarse stage and the second actuator as the fine stage.

The dual actuator system is a dual input single output (DISO) system. This is a subset of the multi-input/multi-output (MIMO) system. All the algorithms applicable to the MIMO systems like the  $H_2$ ,  $H_\infty$  and  $\mu$ -synthesis can be applied. The above mentioned methods often result in higher order controllers. In case of the Master-Slave method [6] each stage is considered to be a single input single output (SISO) system with very little interaction between the two SISO systems. The VCM stage does the coarse positioning while the secondary actuator is used for fine positioning. In reality, there is cross dynamics between the two stages. PQ method [6] takes into consideration the cross-dynamics between the two systems while designing the controller.

## B. Friction Models

Significant effort has gone into modelling friction. The earliest models described a static relation between friction and velocity. A survey of methods to control systems with friction has been conducted by Astrom [4]. Coulomb stated that once the body is in motion friction force is dependent on the direction of velocity and is independent of the velocity magnitude

[7]. Coulomb friction is defined as

$$F = F_c \text{sgn}(v) \quad (2.1)$$

where  $F$  is the friction force,  $F_c > 0$  is the Coulomb friction coefficient and  $v$  the velocity. Systems also encounter viscous friction along with Coulomb friction. Viscous friction varies linearly with the velocity. In equation 2.2,  $F_v$  is the coefficient of viscous friction.

$$F = F_c \text{sgn}(v) + F_v v \quad (2.2)$$

The above model does not describe the friction force when the velocity is zero, since the signum function is not defined at zero. Stiction is the force resisting the movement of the body, when the body is at rest. Friction model for a body with stiction, Coulomb friction and viscous friction is defined as

$$F = \left\{ \begin{array}{ll} F_f & \text{if } v = 0 \text{ and } |F_f| < F_s \\ F_s \text{sgn}(F_f) & \text{if } v = 0 \text{ and } |F_f| > F_s \\ F_c \text{sgn}(v) + F_v v & \text{if } v \neq 0 \end{array} \right\} \quad (2.3)$$

where  $F$  is the friction force,  $F_f$  is the forcing function,  $F_s$  is the stiction force. When the magnitude of forcing function is less than the stiction force, the friction force is equal in magnitude to the forcing function but opposing it. Stribeck proposed that friction force initially decreases as velocity increases from zero and then increases with increasing velocity [8]. Stribeck velocity is the velocity at which friction force is least.



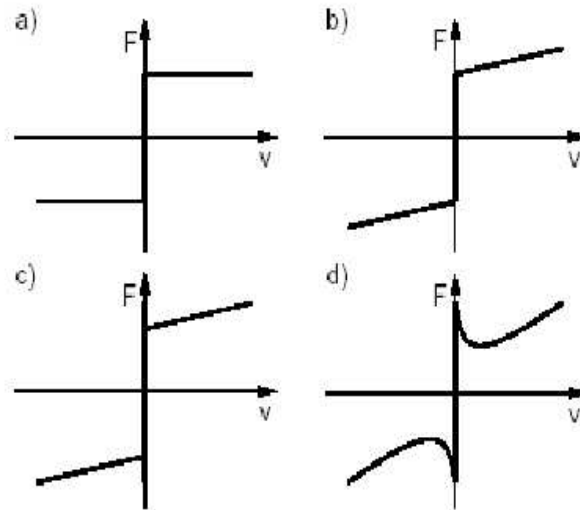


Fig. 2. Static friction models

The various friction models are shown in the Figure 2. Figure 2a depicts a Coulomb friction model. Figure 2b shows a Coulomb friction model along with viscous friction. Figure 2c is a friction model with stiction and Coulomb friction. Figure 2d is the Stribeck friction model.

Static friction models have shortcomings. Friction force computed with the static friction models is discontinuous when the velocity crosses zero. This does not capture the spring like effect due to friction. Also, these models are difficult to implement in simulation due to the transition of friction at zero velocity. In order to overcome this problem, Karnopp [9] proposed a model similar to (2.3). But the condition  $v = 0$  is replaced by  $|v| < \epsilon$ . This is an improvement over static models. The simulation results vary depending on the choice of  $\epsilon$ . A better description of friction is necessary when crossing the zero velocity [2]. The dependency of friction on the position and the acceleration is not considered. Dynamic friction models are able to describe the friction phenomena better when crossing the zero velocity and are also continuous.

Dahl's model described the friction using the stress-strain curve of the material [3]. The surface of solids have microscopic irregularities called as asperities which can be thought of as bristles. Friction between the two surfaces is considered due to interaction between the bristles. Figure 3 shows the interaction between the bristles of the two surfaces. The lower surface, for simplicity sake, is considered to be rigid [2]. The bristles undergo elastic deformation in the stiction region. The force applied is not sufficient for the bristles to deflect completely. When the force applied overcomes stiction, the bristles undergo plastic deformation and bristles deflect permanently. The transition from elastic contact to sliding occurs when the applied force overcomes stiction [10]. According to Dahl, Coulomb friction is related to the interface bond rupture stress between the two surfaces in contact and stiction is related to the ultimate stress of the interface bond. Stiction and Coulomb friction at the interface is related to the elastic and plastic deformation of the asperities respectively. Figure 4 shows the stress-strain curve for a solid material. The region of ultimate stress corresponds to stiction and the "tacky region" where the rupture occurs corresponds to Coulomb friction. A graphical description of the Dahl model is shown in figure 5. The stress-strain curve has been transformed into a force-displacement curve with force being analogous to the stress and displacement to strain [11]. Friction is considered to be a function of position. Since friction is direction dependent it is a function of both velocity and position. Dahl model can be considered to be a Coulomb friction with a lag in the change of friction force when the direction of motion is changed [2].

Dahl's model is given by

$$\frac{dF}{dx} = \sigma \left(1 - \frac{F}{F_s} \operatorname{sgn}(v)\right)^\alpha \quad (2.4)$$

$$\frac{dF}{dt} = \frac{dF}{dx} \frac{dx}{dt} = \sigma \left(1 - \frac{F}{F_s} \operatorname{sgn}(v)\right)^\alpha v \quad (2.5)$$

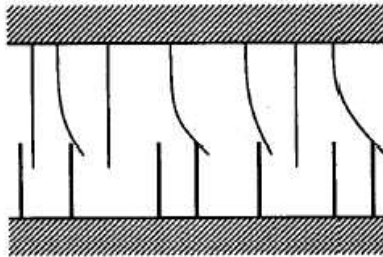


Fig. 3. Interaction between the bristles of two surfaces (Adapted from [2])

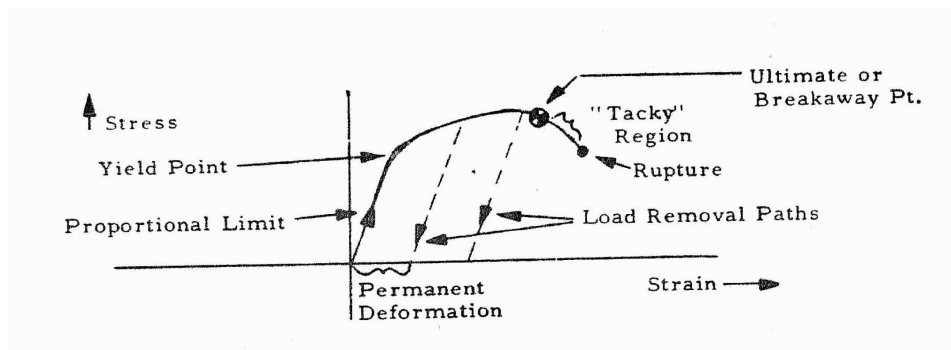


Fig. 4. Stress-strain curve (Adapted from [3])

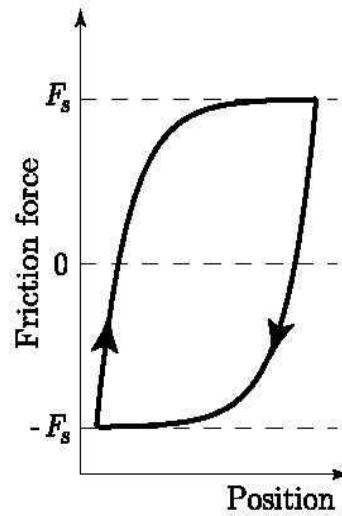


Fig. 5. Dahl model-friction vs position (Adapted from [4])

where  $F$  is the friction force,  $x$  is the displacement,  $\sigma$  is the stiffness coefficient,  $F_s$  is the Coulomb friction force and  $\alpha$  determines the shape of the stress-strain curve. The value of  $\alpha$  is typically assumed to be 1. A sharper stress-strain curve results, when a higher value is assumed for  $\alpha$  [4]. Bliman and Sorine incorporated Stribeck effect into the Dahl model [2]. The time variable in the Dahl model was replaced by the space variable

$$s = \int_0^t |v(\tau)| d\tau \quad (2.6)$$

The model is given by

$$\frac{dF}{ds} = -\sigma_0 \frac{F}{F_c} + \sigma_0 \operatorname{sgn}(v) \quad (2.7)$$

The LuGre model [2] is also an extension of Dahl's model. The friction force is considered to be produced by the spring like behavior of the bristles/asperities. If the applied force is sufficiently large the bristles deflect enough for the slip to occur [12]. It is given by

$$\frac{dz}{dt} = v - \sigma_0 \frac{|v|}{g(v)} z \quad (2.8)$$

$$F = \sigma_0 z + \sigma_1 \frac{dz}{dt} + \sigma_2 v \quad (2.9)$$

where  $z$  denotes the average deflection of the bristles,  $v$  the relative velocity between the two surfaces,  $\sigma_0$  is the stiffness,  $\sigma_1$  is the damping coefficient and  $\sigma_2 v$  accounts for the viscous friction. Function  $g(v)$  is positive and depends on factors such as material properties, lubrication, temperature, etc.

### C. Effect of Friction on Dynamic Systems

Friction plays an important role in the performance of dynamic systems. The system performance is greatly influenced by friction, more so near zero velocity.

The stick-slip motion of a dynamic system is attributed to stiction and Coulomb friction. In case of the stick-slip motion the system alternates between being stationary and moving. The system is stationary when the forcing function is unable to overcome stiction. The system starts slipping once the forcing function is able to overcome stiction. Coulomb friction resists motion during slipping. This motion is akin to the jerky motion of a mass with a spring attached to it. The mass starts moving when it overcomes the spring force and stops momentarily when the spring is compressed. The stick-slip phenomena does not occur if the forcing function is sufficiently larger than stiction force. Figure 6 depicts stick slip motion of a mass subjected to a step input. The step input alternates between 1 Volt and 2 Volt. At lower voltage the mass is unable to overcome stiction force. Sticking phenomena is observed when lower voltage is applied and the mass slips when higher voltage is applied.

Hysteresis occurs due to friction lag in motion control systems. Hysteresis can also

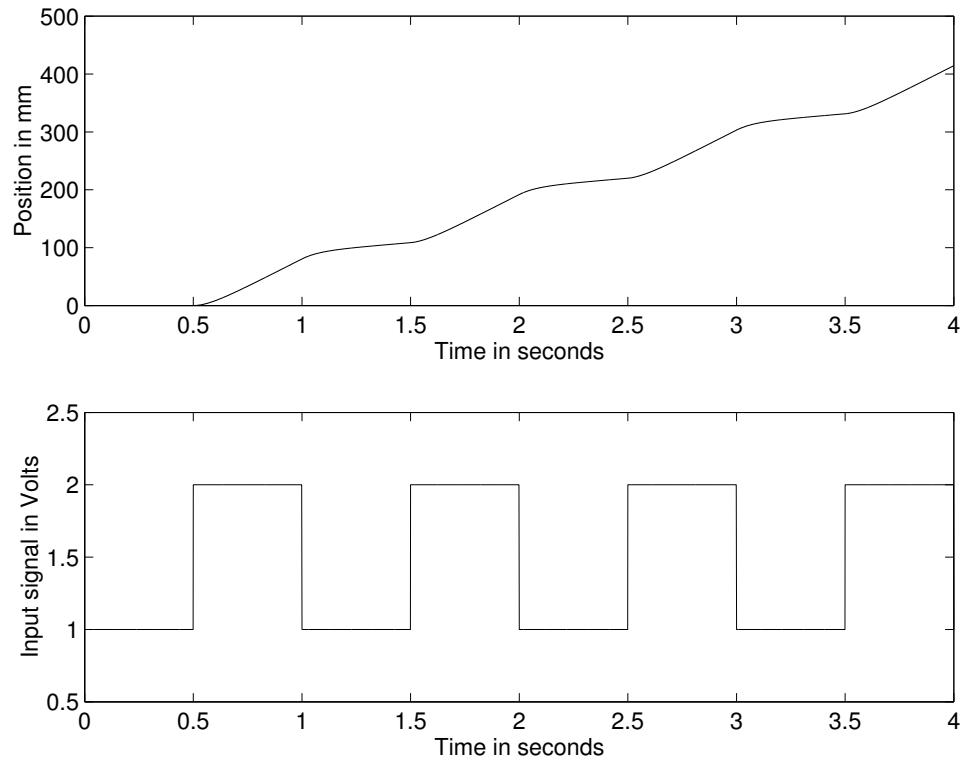


Fig. 6. Stick slip motion of a mass subjected to the above input

be interpreted as system behavior being history dependent. In the Dahl model shown in Figure 5, friction is a function of both position and velocity. In Figure 5, arrows indicate the direction in which the particular segment is active. The direction is directly related to the sign of the velocity. Thus, Dahl model is a function of position and velocity. During the reversal hysteresis is more pronounced since friction force assists motion for a brief period of time.

Friction is an undesirable but an unavoidable phenomena in dynamic systems. Several friction compensation techniques have been developed over the years which try to negate the effects of friction.

Dither is one of the proposed ideas for friction compensation. A fast and small os-

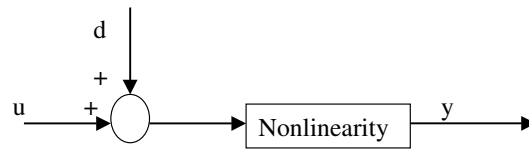


Fig. 7. Schematic of the application of dither signal

cillating motion between bodies in contact eliminates the effect of friction between them and makes the mean effective force zero between the surfaces [13]. The principle of dither being a suitable high frequency signal to the input of the nonlinearity smoothes the nonlinearity [14]. Figure 7 shows a schematic of the application of dither. A high frequency signal,  $d$  is added to the input signal,  $u$  so that the output,  $y$  is linear as regards to the input,  $u$ . Dither can be introduced mechanically or electronically. Friction compensation can also be achieved by acceleration feedback. By closing the feedback loop around the mass it is possible to obtain a high gain loop that controls the acceleration of the mass directly [15]. This technique requires accelerometer. Furthermore, acceleration feedback in conjunction with high gain might destabilize the system.

In case of model based friction compensation, a friction observer is used to estimate the friction in the system [4]. The schematic of a model based friction compensation is shown in Figure 8. The friction observer estimates the friction based on the velocity and position measurements. Additional force equivalent to the estimated friction accounts for friction in the system. Friction model has to be determined beforehand to use this technique, i.e. the model has to be determined offline.

Model based friction compensation is an example of feedback linearization. The central idea of the approach is to algebraically transform a nonlinear system dynamics into a (fully or partially) linear one, so that linear control techniques can be applied [16]. In Figure 8, the loop consisting of friction compensator represents feedback linearization.

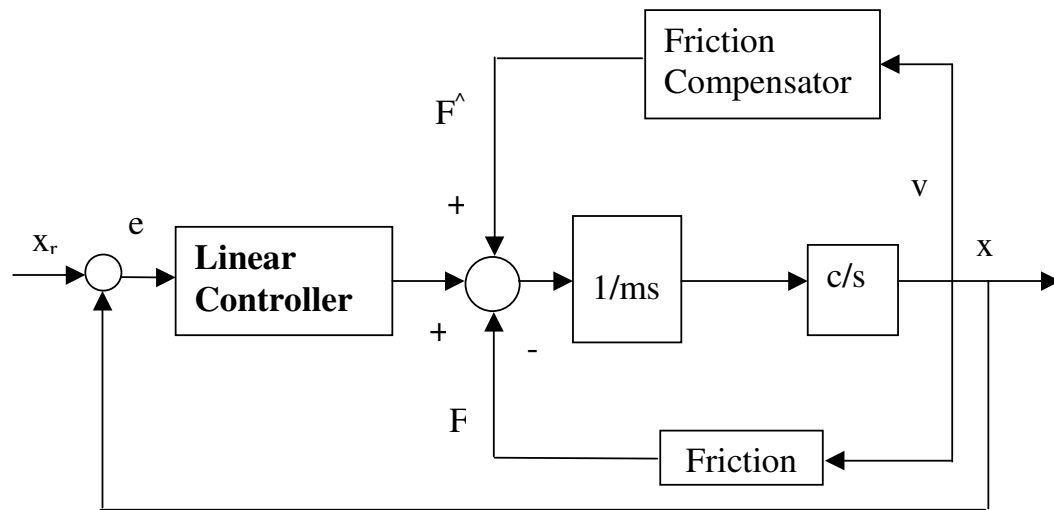


Fig. 8. Model based friction compensation scheme

Feedback linearization does not guarantee robustness in the face of parameter uncertainty or disturbances which have not been modelled.

#### D. System Identification and Modelling

System identification involves identifying the parameters of the system based on certain available information. Usually, the available information is the input/output data set. System identification, in the purview of this thesis, refers to building a mathematical model of the system which satisfactorily predicts the behavior of the system. The three basic entities in system identification are

1. Recording data: Various experiments are to be conducted to obtain a rich input/output data. A rich set of input/output data facilitates modelling of the system for a wide range of conditions. Input signals have to be chosen so as to extract certain information about the system.
2. Model selection and evaluation: Once rich set of input/output data is obtained, the next



step involves choosing a model structure based on certain initial assumptions. The unknown parameters of the chosen model have to be evaluated. In certain cases, standard analysis tools are used to evaluate the model, without choosing any model structure. In such cases, the tools are black boxes as they predict the model based on the input/output data.

3. Validation: The final step of system identification involves validation of the model evaluated in the above step. The model is tested for certain performance criteria and also its behavior is compared with that of the system. Model would be useful if it is able to predict the system behavior with certain accuracy. In case the model fails to predict the system behavior, step 1 and 2 have to be repeated until the model is able to predict the system behavior within acceptable limits.

Parametric identification involves estimation of the parameters for a given model structure. It involves finding the parameters (by numerical search) that minimize the error between the model output and the measured output. In case of non-parametric identification, a model is predicted based on the input/output data without necessarily using a structured model.

## CHAPTER III

### EXPERIMENTAL SETUP

This chapter explains the dual stage actuator test bed in the laboratory. The dual stage actuator test bed in the laboratory consists of a Voice Coil Motor (VCM) mounted on the platform of a slider. The VCM was taken out of a old hard disk drive. The slider is made by Macron Dynamics, Inc. Slider has a travel of 150mm/rev. The overall range of the slider is 0.5m. The slider moves along the rails and is driven by a belt-pulley drive. The dual stage actuator setup is shown in Figure 9.

An arm extends from the VCM, supporting the readhead, which is a part of the linear optical encoder. The linear optical encoder is made by Renishaw. The encoder consists of a readhead, a scale and a interface unit. The readhead is mounted on the tip of the arm. The scale, which is a thin flexible gold plated steel strip, is mounted parallel to the slider. For accurate sensing the gap between the readhead and the scale should be 0.7mm-0.9mm. The output of the interface unit, connected to the readhead by a cable, gives the position information. The linear encoder has a least count of  $0.5\mu\text{m}$ .

The linear range of the VCM arm is +/- 2.5mm. When the motion is imparted to the slider, the arm should remain stationary and centered. In order to keep the arm centered, springs are attached on either side of the arm. Screws are attached to the other end of the springs, using which tension in the springs can be adjusted. There is a set screw on either side of the arm which restricts the arm to operate in the linear range. The VCM along with the arm, sensor, spring-screw attachment constitute the fine stage. The slider along with the belt and pulley form the coarse stage. The motion of the slider is restricted on either ends using contact limit switches.

The fine stage is driven by a servoamplifier, while the coarse stage is driven by a servomotor which in turn is powered by a servodrive. The servomotor and the servodrive

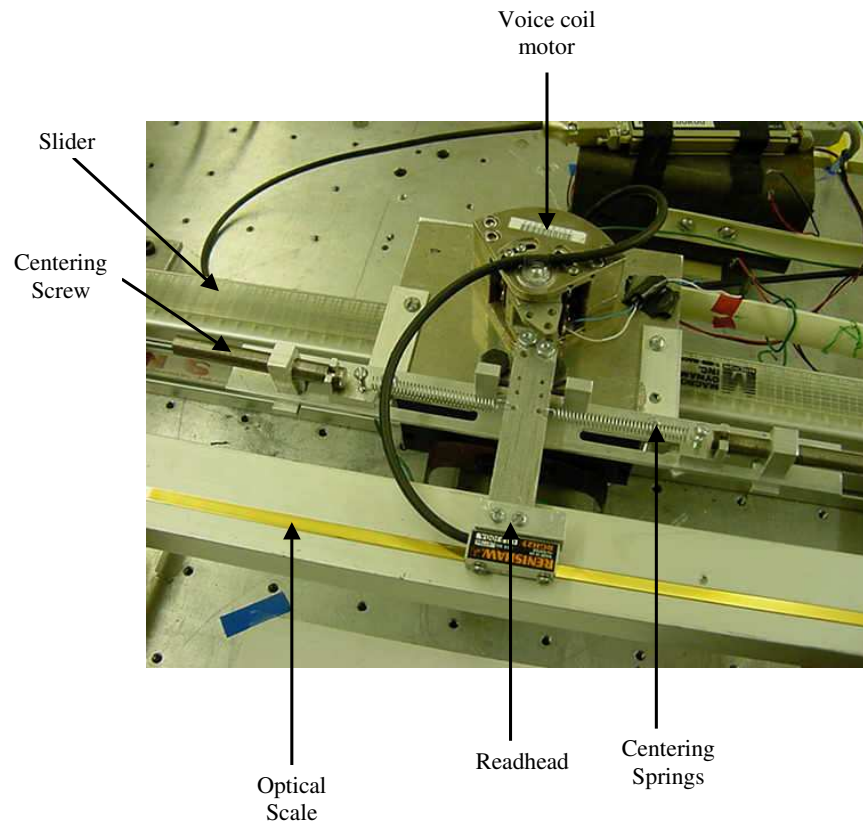


Fig. 9. Dual stage actuator test bed

are from Pacific Scientific and the servoamplifier is from Advanced Motion Controls. The schematic of the dual stage test bed setup is shown in Figure 10. SIMULINK in MATLAB is used for building the models. dSPACE interfaces the Real Time Workshop (RTW) in SIMULINK with the test bed. The whole range of travel (0.5m) of the slider cannot be used since this results in slider hitting the ends. Contact limit switches resist the motion of the slider at either ends. The slider has gradations marked on its side for a span of 270mm. This is the range in which the slider is going to be operated in most cases. The gradations help in determining the absolute position since the position detected by the sensor is relative to the initial(starting) position of the slider.

dSPACE is an extremely powerful package designed for high-speed real-time simulations. Both its hardware and software components are easy to install and ready to perform from simple to complex and multivariable tasks. The hardware consists of a DSP Controller Board based on Texas Instruments TMS320C31 floating-point processor built as a standard PC/AT card that can be plugged into an ISA PC bus. The DS1102 is a stand-alone controller board with various I/O units:

- 4 channels for A/D and D/A conversion,
- 10 digital I/O,
- 6 independent channels for PWM generation,
- one incremental encoder interface
- one hardware interrupt.

The dSPACE software include:

- CONTROLDESK, which is a graphical user interface managing the dSPACE board. It provides the functions for loading, starting and stopping real-time applications on the board.
- Real-Time Library (RTLlib 1102), which includes all functions needed to program the DS1102.

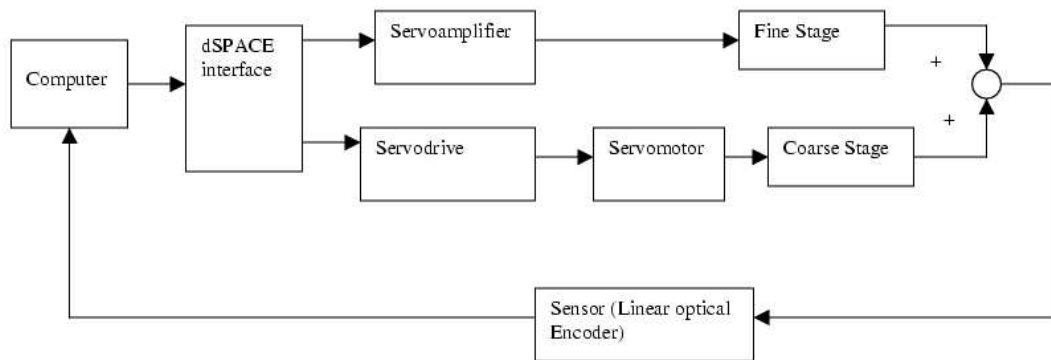


Fig. 10. Block diagram of the dual stage positioning test bed

## CHAPTER IV

### MODELLING

#### A. VCM Model (Fine Stage)

Input/Output data sets were collected for the VCM, so as to model the fine stage. Sinusoidal inputs were used for the fine stage, since frequency response tools were used to identify the fine stage. System identification toolbox in MATLAB was used to find the input/output model for the fine stage. The prediction error method was used to determine the model.

The actual output and the simulated model output were compared. Figure 11 shows the simulated and actual output for a normally distributed random input signal with a zero mean, variance of 0.05 and a zero initial seed. There is an offset between the simulated output and the actual output. When the response of the model and the fine stage were compared for other classes of input, the offset still existed. This can be attributed to modelling errors and also to the fact that the position sensed is not with respect to the absolute index but relative to the starting position. Identified transfer function for the model is

$$\frac{Y(s)}{U(s)} = \frac{1.4s^2 - 4193s - 9.577 \times 10^5}{s^3 + 40.78s^2 + 4015s + 2.589 \times 10^4} \quad (4.1)$$

where  $Y(s)$  represents the output in millimeters and  $U(s)$  represents the input in Volts.

#### B. Coarse Stage

This section describes the modelling of the coarse stage of the dual stage actuator system. One of the main issues in modelling the coarse stage is identification of friction. Various approaches were used for modelling the coarse stage and identifying friction. The following assumptions were made in modelling the coarse stage:

- 1) Servodrive in current mode acts like a gain.

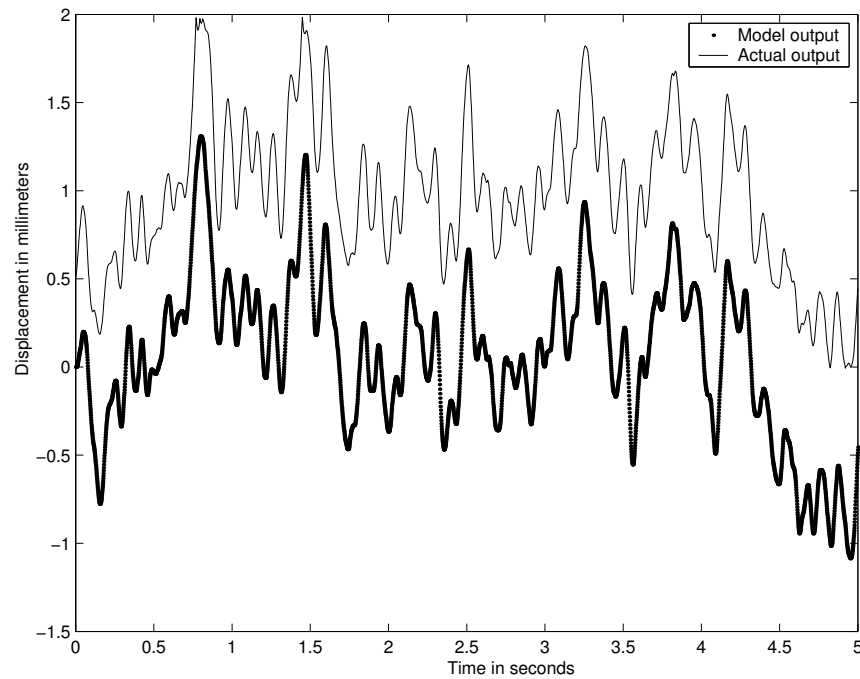


Fig. 11. Comparison of the actual output and the model output for the fine stage

- 2) Belt stiffness is neglected
- 3) No back lash in the gears

Several models were considered for identifying friction. Friction models can be classified as memoryless friction model and friction model with memory. The friction models considered in this thesis for modelling can be broadly listed as

- 1) Coulomb friction model.
- 2) Coulomb friction and stiction model.
- 3) Coulomb friction model dependent on the position of the slider.
- 4) Dynamic model with memory (Dahl model).
- 5) Coulomb friction and Stiction are position and velocity dependent and symmetric with

respect to direction.

6) Friction as a function of position and velocity and also asymmetric with respect to position.

### 1. MATLAB Toolbox

The first step in modelling was to use the system identification toolbox in MATLAB. Prediction error method in MATLAB uses input/output data to determine parameters of a linear model. This method was used to model the fine stage. Neither the structure nor the order of the system needs to be specified. Zero mean sinusoidal and other periodic input signals were used to generate the Input/Output data. The linear model determined by the toolbox did not satisfactorily predict the behavior of the slider.

### 2. Parametric Modelling

The next step was to try estimating the parameters of the model, assuming a structure. The parameters were calculated using the least squares algorithm. The following structure was used to determine the parameters.

$$m\frac{d^2x}{dt^2} + c\frac{dx}{dt} + F_c\text{sgn}\left(\frac{dx}{dt}\right) = F_{applied} \quad (4.2)$$

where  $m$  is the mass of the slider,  $c$  is the damping coefficient and  $F_c$  is the Coulomb friction constant and  $x$  the displacement.  $F_{applied}$  represents the lumped forcing function acting on the slider. This model did not take into account the effect of stiction. The dynamics of the servodrive and the servomotor were neglected. The lumped forcing function was calculated assuming the servomotor actuator, driving the slider, along with the servodrive, as a gain.

The unknown parameters are mass of the slider, damping coefficient and Coulomb



friction coefficient. The known information from the experiments is the slider position and the force at each time instance. The velocity and the acceleration are estimated by filtering and numerically differentiating the position. The calculated acceleration and velocity are denoted by  $\hat{a}$  and  $\hat{v}$  respectively. The following set of equations represent the differential equation.

$$\begin{pmatrix} a(\hat{t}_1) & v(\hat{t}_1) & \text{sgn}(v(\hat{t}_1)) \\ a(\hat{t}_2) & v(\hat{t}_2) & \text{sgn}(v(\hat{t}_2)) \\ \vdots & \vdots & \vdots \\ a(\hat{t}_n) & v(\hat{t}_n) & \text{sgn}(v(\hat{t}_n)) \end{pmatrix} \begin{pmatrix} m \\ c \\ F_c \end{pmatrix} = \begin{pmatrix} F_{applied}(t_1) \\ F_{applied}(t_2) \\ \vdots \\ F_{applied}(t_n) \end{pmatrix} \quad (4.3)$$

The unknowns ( $m, c, F_c$ ) which achieve the best possible fit to the above set of equations was determined. Mass ( $m$ ) was estimated to be 3.4Kg, Coulomb friction coefficient ( $F_c$ ) to be 4.5N and the damping coefficient( $c$ ) to be 45Ns/m. The above structure was not able to capture the behavior of the system satisfactorily in simulation. The forcing function used to gather data was sinusoidal waves. Figure 12 shows the comparison of the actual output and the simulated output, at steady state, for a sinusoidal input of amplitude 3V and 4Hz frequency. The amplitude of the response is comparable. This comparison is for a particular initial condition of the slider. Comparing the responses for a more generic signal will help validate the model better. Figure 13 shows the actual output vs the simulated output for a zero mean, band limited, white, Gaussian noise. The amplitude of response in simulation is much larger than that of the actual system.

While comparing the simulation response with the actual output, there is a phase difference between the two. This is due to the fact that the simulation and the experiment were not conducted simultaneously. While conducting the experiments, the data capture (and also the motion of the slider) does not begin at  $T = 0$  since data capture settings have to be configured before capturing the data. This leads to input signal being non-zero when

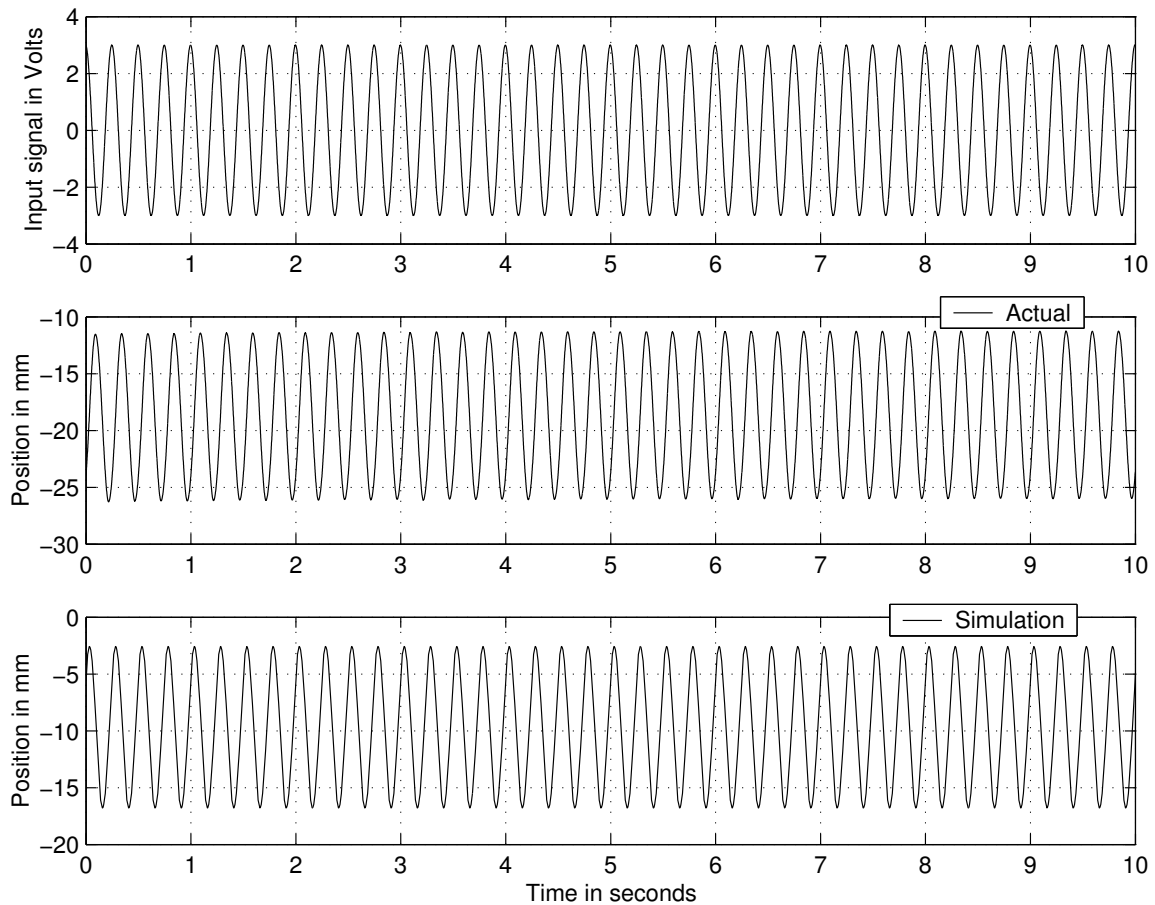


Fig. 12. Comparison of the actual output and the model output, at steady state, for the coarse stage considering Coulomb friction

the data capture (and motion of the slider) starts.

### 3. Coulomb Friction and Stiction Model

The above structure tried to explain the non-linearity in the system by assuming Coulomb friction. It did not consider the fact that the system also has to overcome stiction when starting from rest. This model tries to capture stiction behavior of the system. In order to determine stiction, a constant voltage signal, which translates to a constant force, was

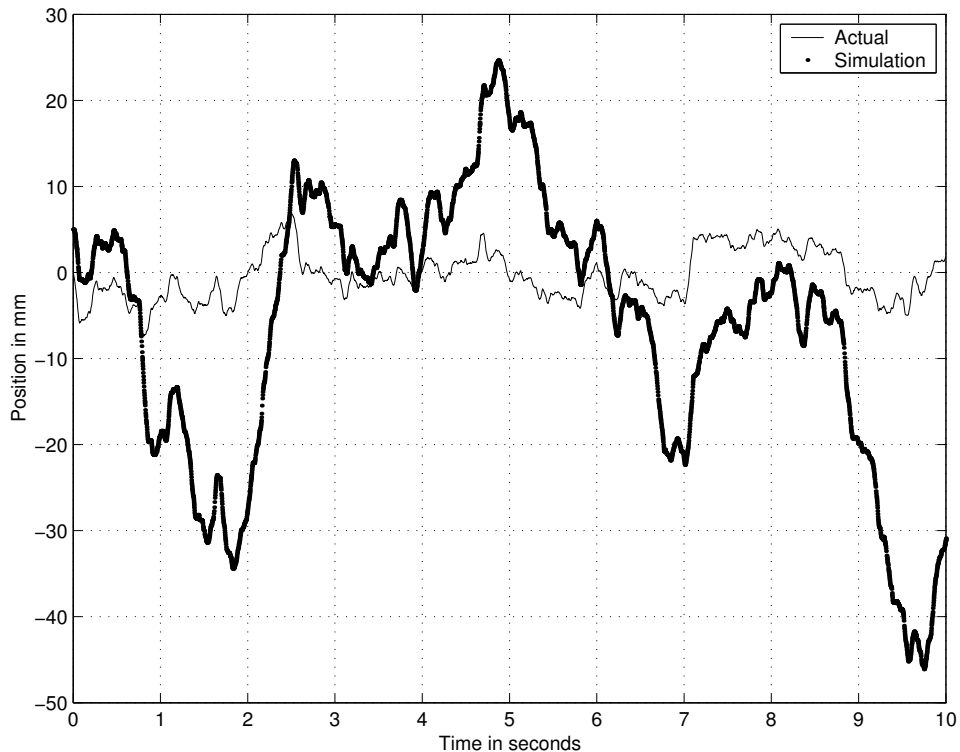


Fig. 13. Comparison of the actual output and the model output, input being zero mean, white Gaussian noise, for the coarse stage considering Coulomb friction

applied on the slider. The slider does not move until a threshold voltage, which overcomes stiction, is applied. The voltage( correspondingly current too) was increased gradually till the slider started moving. The current required to move the slider is around 1A. The Coulomb friction coefficient is assumed to be half of the magnitude of stiction. Figure 14 denotes the comparison between the model output and the actual output at steady state. Figure 15 depicts the actual output vs the simulated output for a zero mean, band limited, white, Gaussian noise. The model output qualitatively matches the actual output better as compared to the previous model.

While collecting sets of input/output data for further analysis several phenomena were observed. They were:

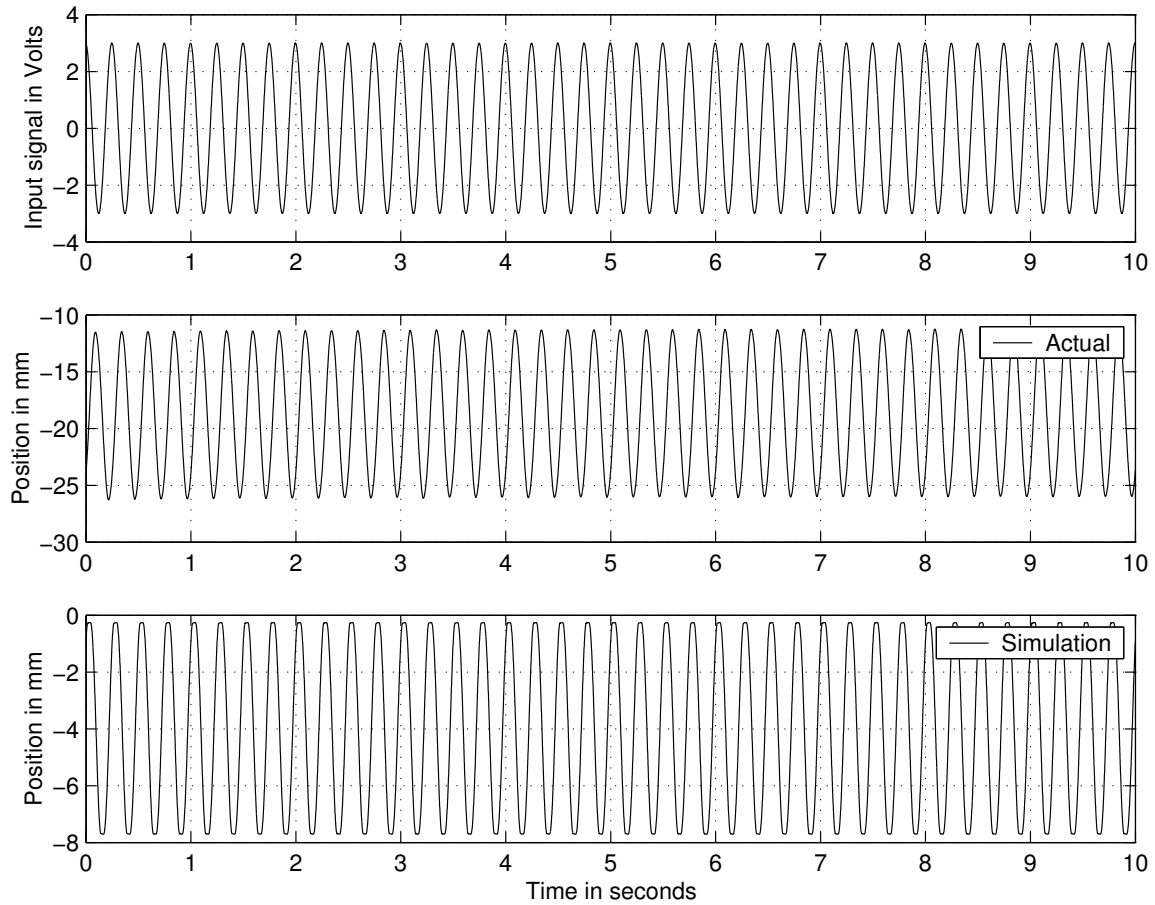


Fig. 14. Comparison of the actual output and the model output, at steady state, for the coarse stage considering Coulomb friction and stiction

- 1) In the open loop, the slider drifts from its mean position towards the center when excited with zero mean periodic signals.
- 2) Slider moves by a certain magnitude when a constant amplitude signal is applied. When the input signal is reversed, the slider moves by a larger magnitude.

The Coulomb and stiction model had shortcomings in predicting the drift of the system in open loop, when excited with zero mean, periodic signals. The slider was excited with

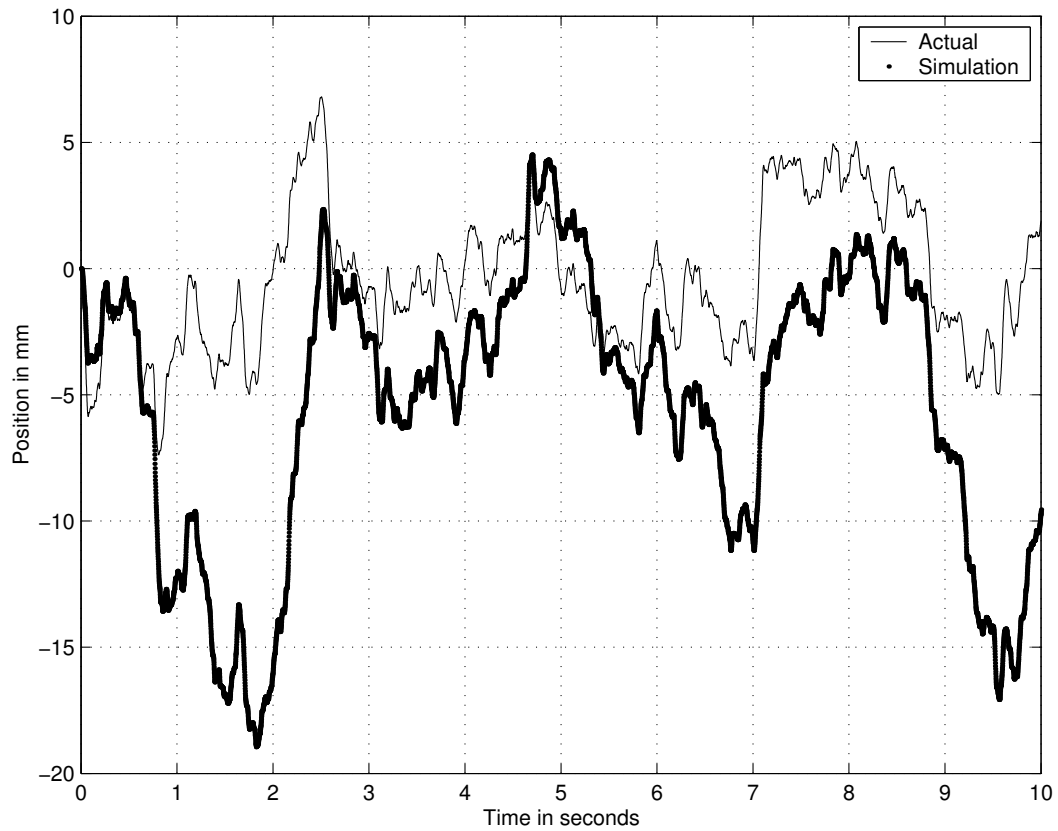


Fig. 15. Comparison of the actual output and the model output with zero mean, white Gaussian noise as the input for the coarse stage, considering Coulomb friction and stiction

sinusoidal input signals of varying frequency in order to capture the frequency response behavior and the bandwidth of the slider. When operated in open loop, with zero-mean sinusoidal input signal, the slider exhibited tendency to drift towards the center irrespective of the initial position. Figure 16 shows the drift of the slider in the open loop for a zero mean sinusoidal input signal, when the initial position was at the left end (10mm) of the slider. Figure 17 shows the drift of the slider in the open loop for a zero mean sinusoidal input signal, when the initial position was at the right end (205mm) of the slider.

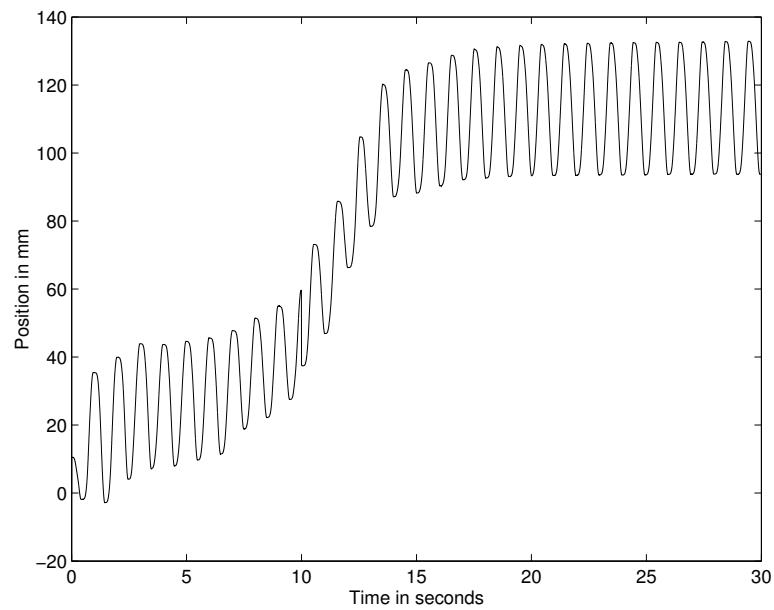


Fig. 16. Drift of the slider in the open loop when starting from the left end (10mm)

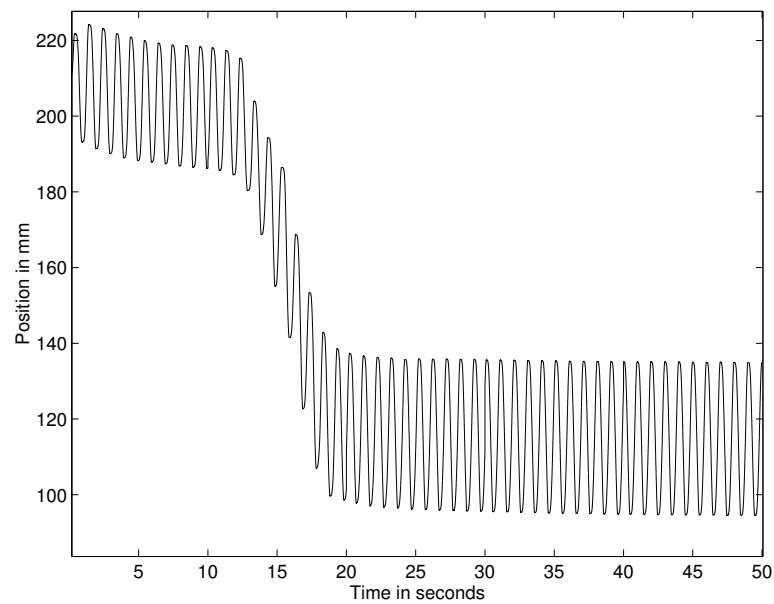


Fig. 17. Drift of the slider in the open loop when starting from the right end (205mm)

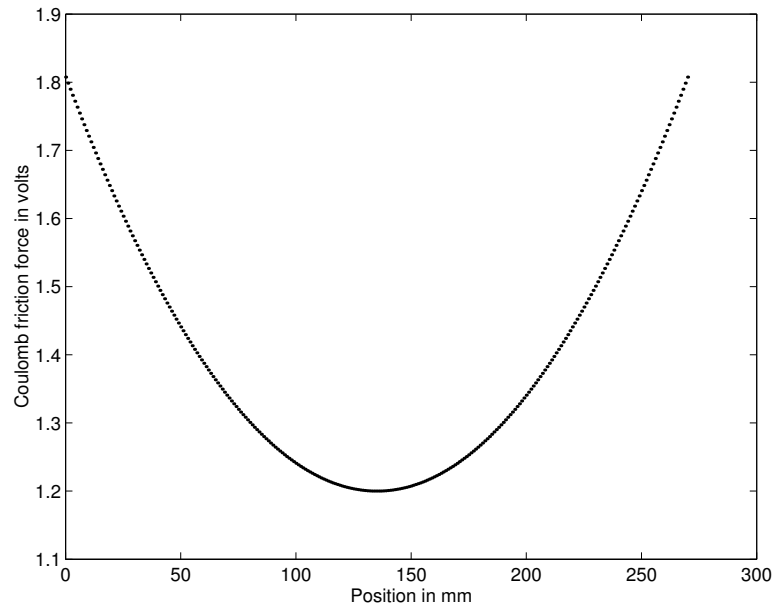


Fig. 18. Parabolic friction map

#### 4. Position Dependent Friction Model

One of the observations made while trying to model friction was that the force required to move the slider from rest at different locations along the slider, varies. This emphasizes that the resistance to motion varies along the length of the slider. Open loop response of the slider gives an insight into the behavior of the system. This phenomena was assumed to be due to varying Coulomb friction along the length of the slider. To test the hypothesis, a position dependent Coulomb friction map was assumed. The Coulomb friction was assumed to be lowest at the center and largest at the ends. The value of Coulomb friction at the ends and at the center was assumed based on the input signal required to move the system from rest at those locations. The parabolic friction map is shown in Figure 18. Karnopp model [9] was used to describe the stiction at zero-crossing.

Using the above friction map, the open loop simulation results were verified against

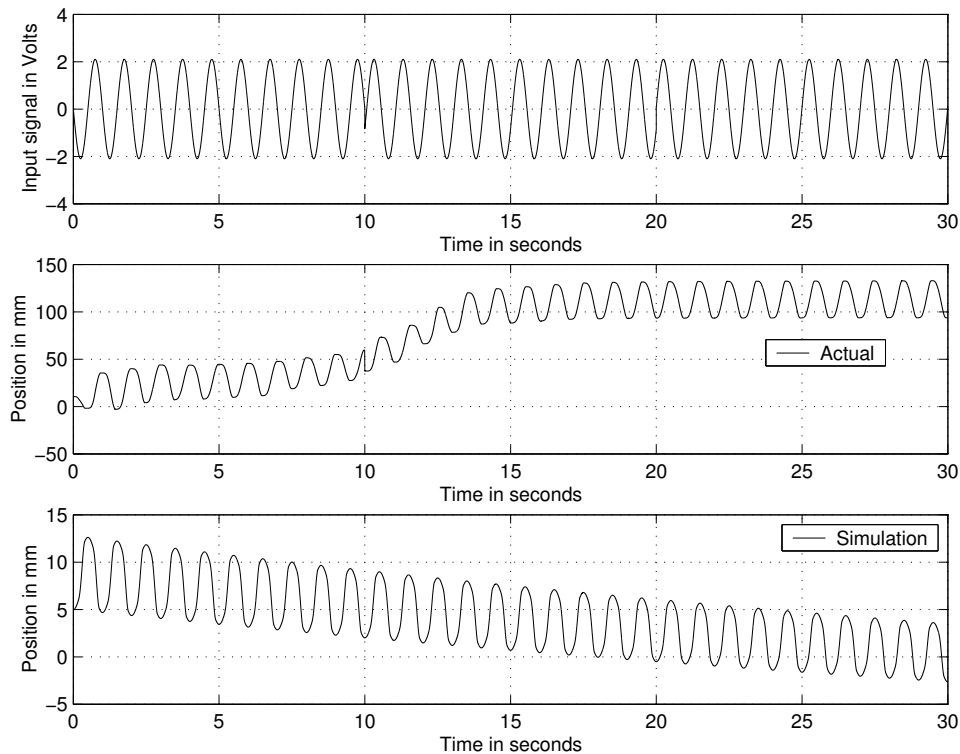


Fig. 19. Comparison of the actual and model output for a sinusoidal signal considering Coulomb friction to be parabolic

the experimental data. Figure 19 shows the response of the system and the model for a sinusoidal input signal. The drift in the simulation is opposite in direction to that of the drift occurring in the system. An inverse parabolic function map (i.e. friction being largest at the center and lowest at the ends) was considered since the drift in the model was in the opposite direction. The open loop simulation results for the above case too did not capture the correct nature of the drift of the slider.

## 5. Model Considering the Drive Train

Until now all the models considered did not take into account the dynamics of the motor, servodrive or the belt drive system. Motor, servodrive and belt drive systems were treated



as a simple gain. The behavior of the slider is influenced by the motor dynamics, stretching of the belt, etc. The influence of the motor dynamics and other phenomena were considered to be negligible. The new model takes into account all these elements. The Bond graph methodology was used for modelling the complete system. This model included the belt stiffness and the dynamics of the motor and the gears. The state space model is given by the below set of equations.

$$\begin{pmatrix} \ddot{\theta} \\ \dot{T} \\ \ddot{x} \end{pmatrix} = \begin{pmatrix} \frac{-R_b}{J_m + r^2 I_g} & \frac{-r}{J_m + r^2 I_g} & 0 \\ K_b r & 0 & -K_b \\ 0 & \frac{1}{m} & -\frac{C_v}{m} \end{pmatrix} \begin{pmatrix} \theta \\ T \\ x \end{pmatrix} + \begin{pmatrix} \frac{K_t}{J_m + r^2 I_g} \\ 0 \\ 0 \end{pmatrix} S_f \quad (4.4)$$

where  $\theta$  is the angular displacement of the rotor,  $T$  is the tension in the belt,  $x$  is the displacement of the slider,  $R_b$  is the bearing friction,  $J_m$  is the inertia of the motor,  $I_g$  is the inertia of the gear,  $r$  is the mean radius of the pulley,  $K_b$  is the belt stiffness,  $m$  is the mass of the slider,  $C_v$  is the damping coefficient of the slider,  $K_t$  is the torque constant and  $S_f$  is the forcing function.

Nominal values were assumed for mass ( $m$ ) and damping coefficient ( $C_v$ ) of the slider and the belt stiffness ( $K_b$ ). The values of bearing friction ( $R_b$ ), motor inertia ( $J_m$ ), gear inertia ( $I_g$ ), mean radius of the pulley ( $r$ ) and torque constant ( $K_t$ ) were noted from the specifications. Friction components are included in the first and the third equation. Friction is assumed to be present both in the slider and the motor. Figure 20 shows the actual output and the simulation output for a zero mean, sinusoidal input signal. The model is not able to predict the drift in the system. In the above model, the friction force is not a function of position. Friction is proved to be a function of position in the later part of the thesis. Also, at zero crossing the friction force is assumed to be a linear function of velocity with a very high slope.

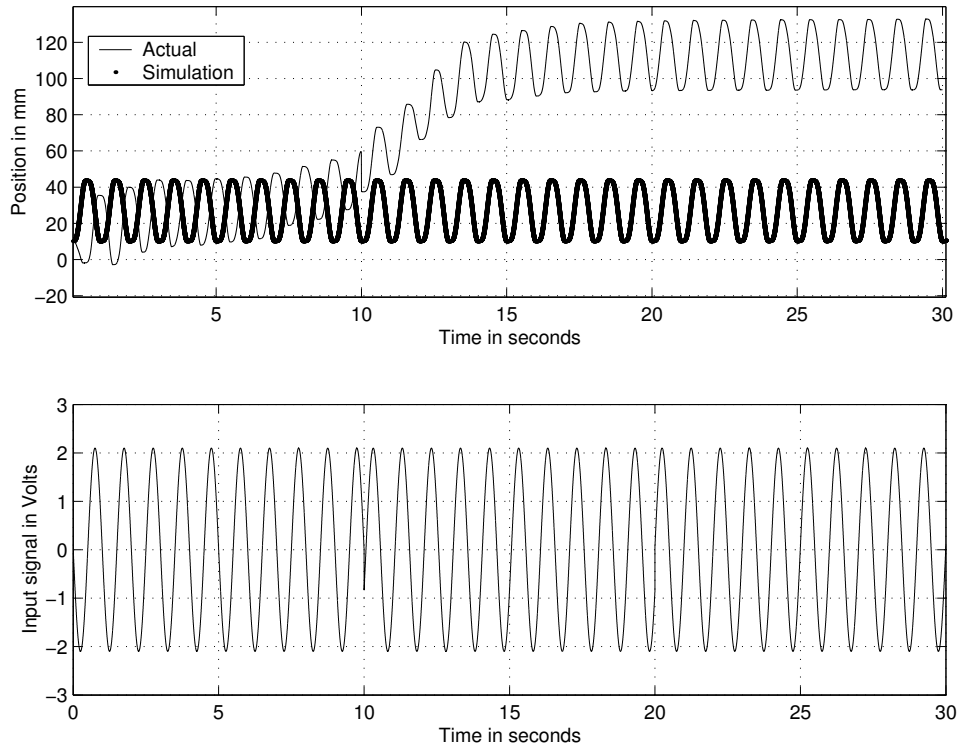


Fig. 20. Comparison of the simulation and the actual output for a zero mean sinusoidal input signal considering drive train model

## 6. Dynamic Model with Memory

Memoryless friction models have shortcomings. Friction force computed with the memoryless friction models is discontinuous when the velocity crosses zero. A better description of friction is necessary when crossing the zero velocity. The dependency of friction on the position and the acceleration is not considered. Dynamic friction models are able to better describe the friction phenomena when crossing the zero velocity and are also continuous. Dahl model is one of the dynamic models.

Dahl's model is given by

$$\frac{dF}{dx} = \sigma \left(1 - \frac{F}{F_s} \text{sgn}(v)\right)^\alpha \quad (4.5)$$

$$\frac{dF}{dt} = \frac{dF}{dx} \frac{dx}{dt} = \sigma \left(1 - \frac{F}{F_s} \text{sgn}(v)\right)^\alpha v \quad (4.6)$$

where  $F$  is the friction force,  $x$  is the displacement,  $\sigma$  is the stiffness coefficient,  $F_s$  is the Coulomb friction force and  $\alpha$  determines the shape of the stress-strain curve. The value of  $\alpha$  is typically assumed to be 1. A sharper stress-strain curve results, when a higher value is assumed for  $\alpha$ .

Simulations were run assuming the friction model to be Dahl model. The response of the simulations to sinusoidal input signals was compared with the response of the slider to the same signals. The simulated output didn't match the experimental output qualitatively. Figure 21 shows the comparison of the actual output and the simulated output for a sinusoidal input signal. The amplitude of response in simulation is less than the actual magnitude. The simulated response does not show any drift characteristics. In case of Dahl model, as shown in Figure 5, the friction force is direction dependent. As noted earlier, Dahl model is considered to be a Coulomb friction model which captures the hysteretic behavior while changing the direction of motion [2]. Friction in the coarse stage of the test bed under consideration is asymmetric with respect to position, which is not captured by the Dahl model.

## 7. Estimation of the Linear Parameters

The structure considered to model the coarse stage is shown in the equation below.

$$m \frac{d^2x}{dt^2} + c \frac{dx}{dt} + F = F_{applied} \quad (4.7)$$

where  $m$  is the mass of the system,  $c$  is the damping coefficient,  $F$  represents the non-

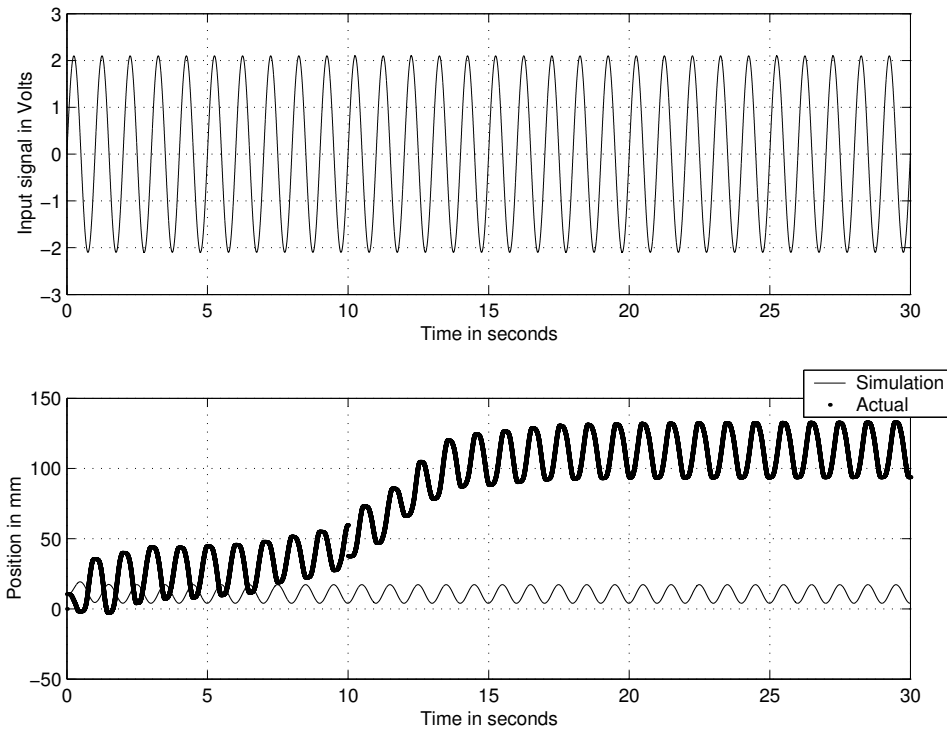


Fig. 21. Comparison of the simulation and the actual output for a zero mean, sinusoidal input signal, considering Dahl model

linear friction force and  $F_{applied}$  is the input signal. The linear parameters in the above equation are  $m$  and  $c$ . The linear parameters of the system can be estimated without estimating the friction. If a square wave of a magnitude much greater than the friction force is chosen to excite the system, system behavior is close to that of a linear system [17]. The system equation can be approximated by

$$m \frac{d^2x}{dt^2} + c \frac{dx}{dt} \simeq F_{applied} \quad (4.8)$$

This can also be written in the Laplace domain as

$$ms^2X(s) + csX(s) \simeq F_{applied} \quad (4.9)$$

By using a stable filter  $\lambda(s)$  the above equation (4.9) becomes

$$ms^2 \frac{X(s)}{\lambda(s)} + cs \frac{X(s)}{\lambda(s)} \simeq \frac{F_{applied}}{\lambda(s)} \quad (4.10)$$

$$\begin{pmatrix} s^2 \frac{X(s)}{\lambda(s)} & s \frac{X(s)}{\lambda(s)} \end{pmatrix} \begin{pmatrix} m \\ c \end{pmatrix} \simeq \begin{pmatrix} F_{applied} \\ \lambda(s) \end{pmatrix} \quad (4.11)$$

$$\begin{pmatrix} u_1(t_1) & u_2(t_1) \\ u_1(t_2) & u_2(t_2) \\ \vdots & \vdots \\ u_1(t_n) & u_2(t_n) \end{pmatrix} \begin{pmatrix} m \\ c \end{pmatrix} \simeq \begin{pmatrix} F_{filter}(t_1) \\ F_{filter}(t_2) \\ \vdots \\ F_{filter}(t_n) \end{pmatrix} \quad (4.12)$$

where  $u_1 = s^2 X(s)/\lambda(s)$ ,  $u_2 = sX(s)/\lambda(s)$  and  $F_{filter} = F_{applied}/\lambda(s)$ .  $u_1$ ,  $u_2$  and  $F_{filter}$  are known. The unknowns ( $m$ ,  $c$ ) which achieve the best possible fit for the above set of equations was determined. This gives the estimate of the linear parameters. In order to choose the magnitude of the signal, the system was excited with a set of square waves of different magnitudes but same frequency. For a linear system, the gain of the system remains constant at any particular frequency. Therefore the ratio of the outputs should be equal to the ratio of inputs. The set of square waves which led to the closest match of the ratio of inputs to the ratio of outputs was used to estimate the linear parameters of the system. For the set of square waves with magnitude 6V and 6.5V and frequency 2Hz the ratio of outputs and the ratio of inputs was 0.9231 and 0.9333, respectively. Using the data captured with this set of square waves in equation (4.12), the value of the lumped mass( $m$ ) of the coarse stage was determined to be 3.5Kg and the damping coefficient( $c$ ) to be 30Ns/m.

### C. Summary of experiments

As mentioned earlier, data collection is an important aspect of identification of friction. A rich set of input/output data encompassing various frequencies of input signal along with the response of the system at various locations gives a good idea about the resistive forces. Various experiments were designed to collect rich sets of input/output data. Each of these experiments tried to capture a particular behavior of the slider.

#### 1. Random Triangular Signal

In order to develop a position dependent friction model the input/output data had to be collected for many different coarse actuator positions. To drive the system back and forth along the axis, an intermittently non-zero input signal was used. The non-zero segment of the input signal was a triangular wave with random amplitude and random period. Direction of the forced motion changed once the slider touched the limit switches. Over a period of time rich sets of input/output data was collected. The system started from rest for every wave generated and had to overcome stiction in every cycle. An example of the triangular random input signal is shown in Figure 22.

#### 2. Hysteresis/Asymmetry

The slider has a limited range of motion. The operating range of the slider spans 270mm. The forcing function changes its sign once the slider reaches the extreme ends. The change in sign is achieved by setting software limits for the range of motion. In Figure 23, the slider is excited with a constant amplitude (2.5V) triangular wave with a period of 3s. The forcing function changes sign once the slider reaches 270mm or 0mm. Once the forcing function changes direction, the magnitude of displacement is larger as compared to when the slider was moving in the same direction. This difference in magnitude of displacement

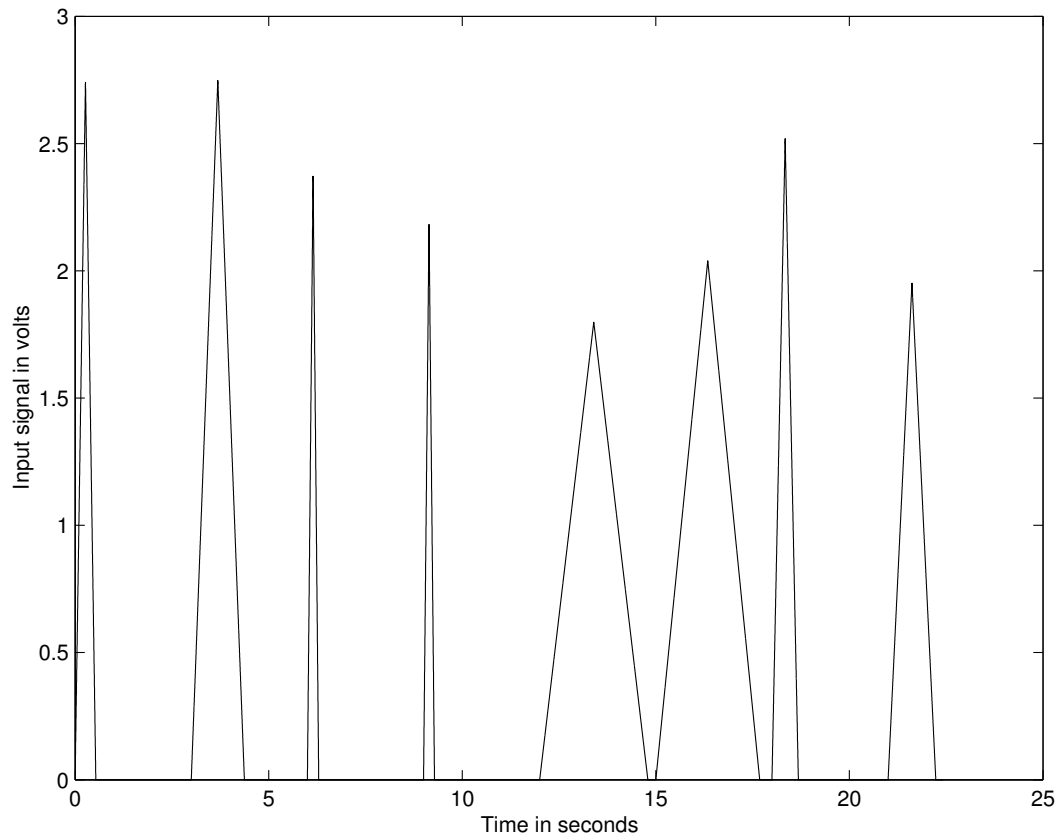


Fig. 22. Random triangular input signal

for a constant amplitude signal is due to hysteresis.

An experiment was designed to test the slider for hysteretic/drifted behavior. The drifting was attributed to the asymmetrical, direction dependent, friction. The experiment recorded the displacement of the slider from a fixed test point. The slider was made to reach the test point from either side of the test point. After reaching the test point the slider was made to move in either direction. The four test cases are

- The slider would reach the test point from the left side and continue moving in the same direction.
- The slider would reach the test point from the left side and move in the opposite direc-

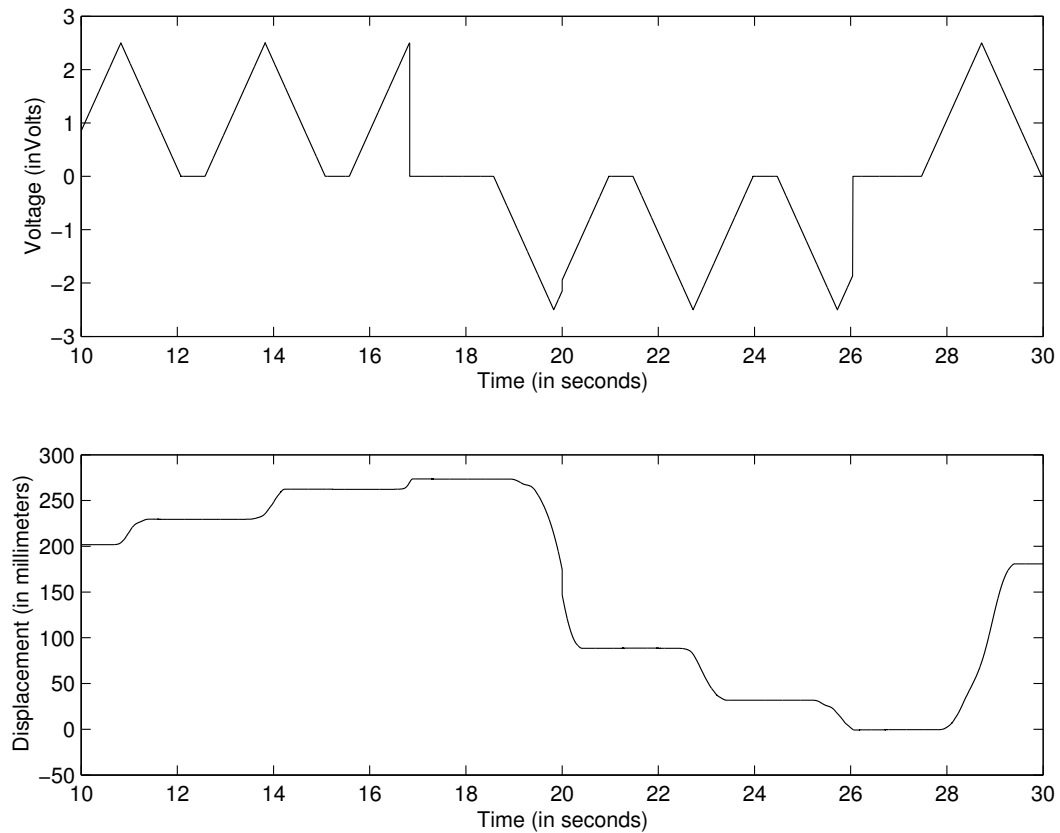


Fig. 23. Displacement of the slider with the forcing function

tion.

- The slider would reach the test point from the right side and continue moving in the same direction.
- The slider would reach the test point from the right side and move in the opposite direction.

The experiment was conducted at two test points roughly at quarter the length from the ends.

Figure 24 depicts the displacement of the slider for various forcing conditions. Irrespective of how the slider reached the test point, the displacement was larger when moving



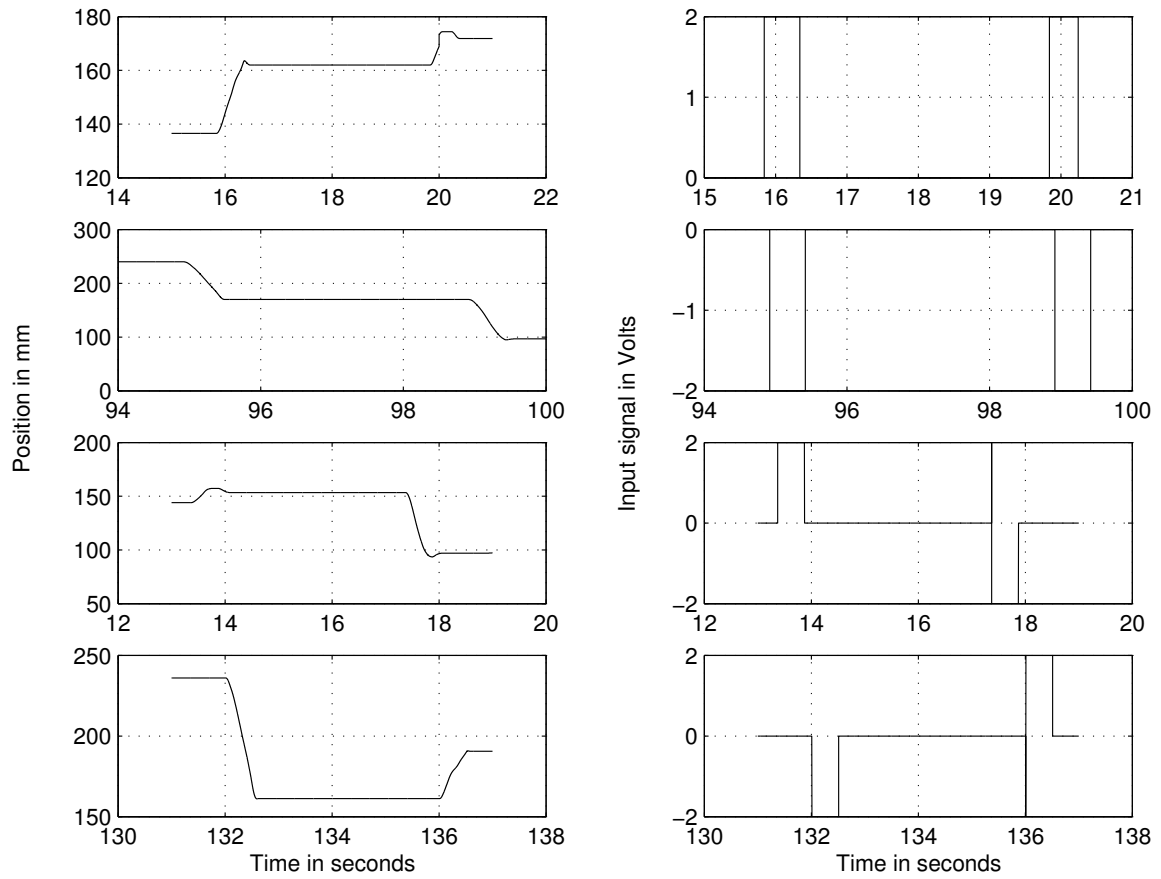


Fig. 24. Displacement vs voltage: different cases

towards center. Thus, it displays a predominant asymmetric behavior as compared to hysteretic behavior. When the above experiment was repeated with test point being on the other side of the center, the displacement was still larger when slider moved towards the center. This reiterates the drifting behavior of the slider.

### 3. Velocity Limit Experiment

Another experiment forced the slider to move between certain velocity limits. When the slider reached a certain velocity, a lower voltage was applied to slow down the slider and when the slider slowed down to a certain velocity, a higher voltage was applied to force it move faster. The central idea was to force the system to move at constant velocity by bringing the limits closer. Maintaining a constant velocity would eliminate the acceleration term from the system equation (4.7). Thus, knowing the input signal, velocity and coefficient of damping, friction force can be calculated. Figure 25 is an example of the velocity based experiment. The upper limit is set at 40mm/s and the lower limit at 10mm/s. This made the slider accelerate and decelerate, alternatingly. This could not be implemented to maintain a constant velocity since tighter limits could not be imposed due to phase lag in estimation of velocity.

#### D. Position and Direction Dependent Models

The models considered until this point were either static friction models or dynamic model which incorporated position dependency. A friction model which is dependent on position and direction has not been considered. The drift of the slider, towards the center, in open loop for zero mean periodic signals could be attributed to friction force which is direction and position dependent. Friction force is assumed to be decreasing towards the center. Based on this assumption a position and direction dependent friction model was

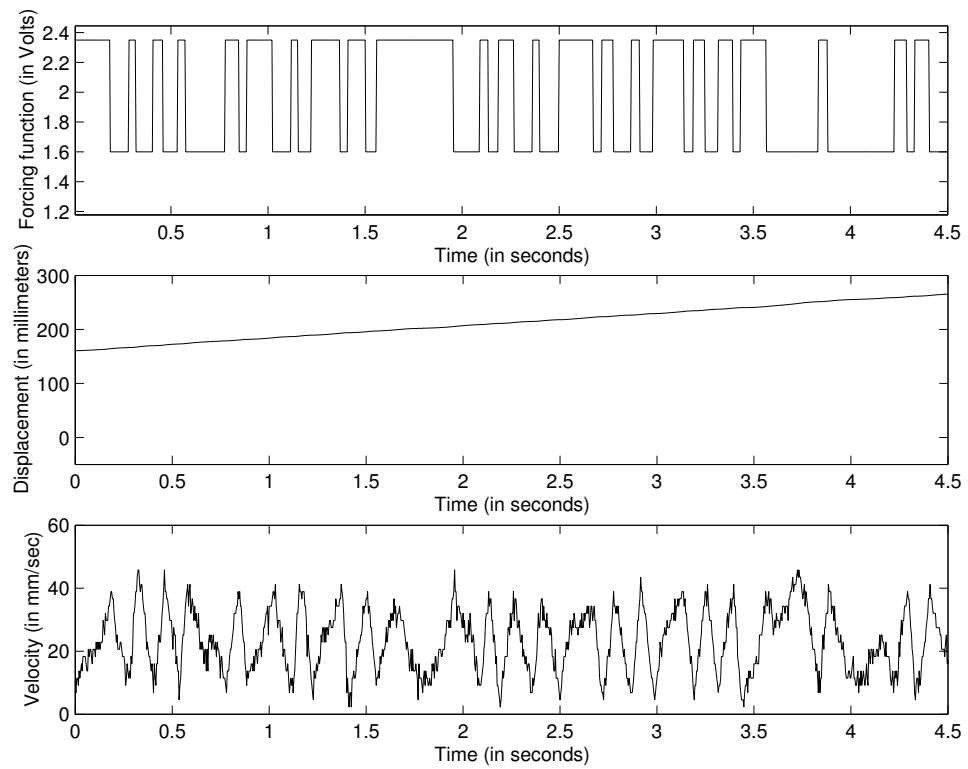


Fig. 25. Velocity limit experiment

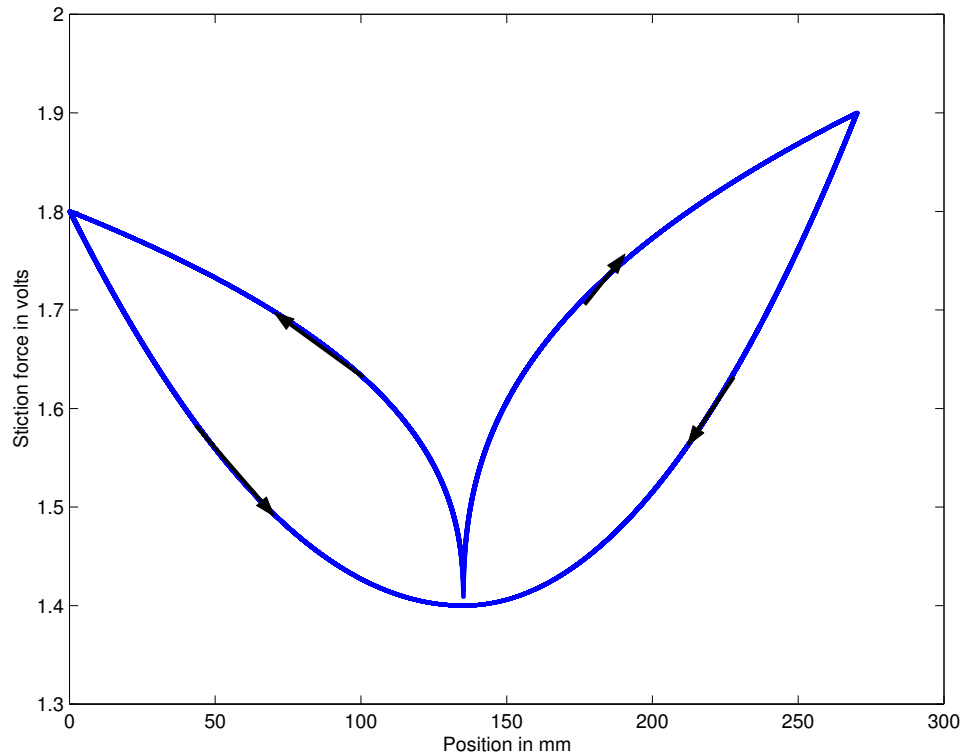


Fig. 26. Direction and position dependent stiction model

constructed. Figure 26 shows stiction force as a function of position and direction. The arrows indicate the direction in which the particular segment is considered. If the slider is moving from left end towards the center friction force is considered to be lesser, than when it is moving in the opposite direction. When the slider crosses the mid point and tries to move away from the center friction force increases. The variation of Coulomb friction force with respect to position and direction is assumed to be similar to the variation of stiction force but lesser in magnitude. This assumption is based on the description of Coulomb friction in static friction models.

The simulation output and the actual output were compared for a set of initial conditions. The input signal was a zero mean sinusoidal signal of amplitude 2.1V and 1Hz

frequency. The figure 27 shows the simulated response and the response of the coarse stage to the above described input signal. The difference in the phase between the simulation result and the actual output is due to the fact that the data capture of experiments do not start at time  $T = 0$  as explained at the start of this chapter. Author is more interested in comparing the magnitude and the nature of response to input signals of equal magnitude. The second part of Figure 27 shows the comparison of responses when the initial condition of the slider is 10mm. The third part of Figure 27 shows the comparison of responses when the initial condition of the slider is 210mm. In both the cases drift predicted by the model, although similar to drift of the slider, occurs faster in simulation as compared to the response of the actual system. This is more true when the slider is drifting from the right end towards the center. Although drift predicted by this model does not match drift of the slider, the promising thing to be noted here is that the model is able to predict drift of the slider in open loop when subjected to zero mean periodic signals.

In the stiction model mentioned above, input signal required to move the system from rest was experimentally determined at a few salient locations (at the ends and at the center). The profile of stiction in between regions was extrapolated assuming the variation of stiction along position to be a smooth higher order function. Figure 28 shows the response of the slider to a periodic input signal which is 4.75V for 0.05s and zero for the next 0.75s. The slider traverses the entire range considered from 0-270mm and back. The slider traverses by varying amplitude for the above applied constant signal. This suggests that force opposing the motion varies along the length of the slider. In order to model friction better as compared to the previous models, the variation of stiction force along the length of the slider has to be better captured. This would also give an insight into the nature of opposing force along the slider.

An experiment was designed to capture the force required to move the slider from rest along the length of the slider. Stiction force would be captured as a function of position.

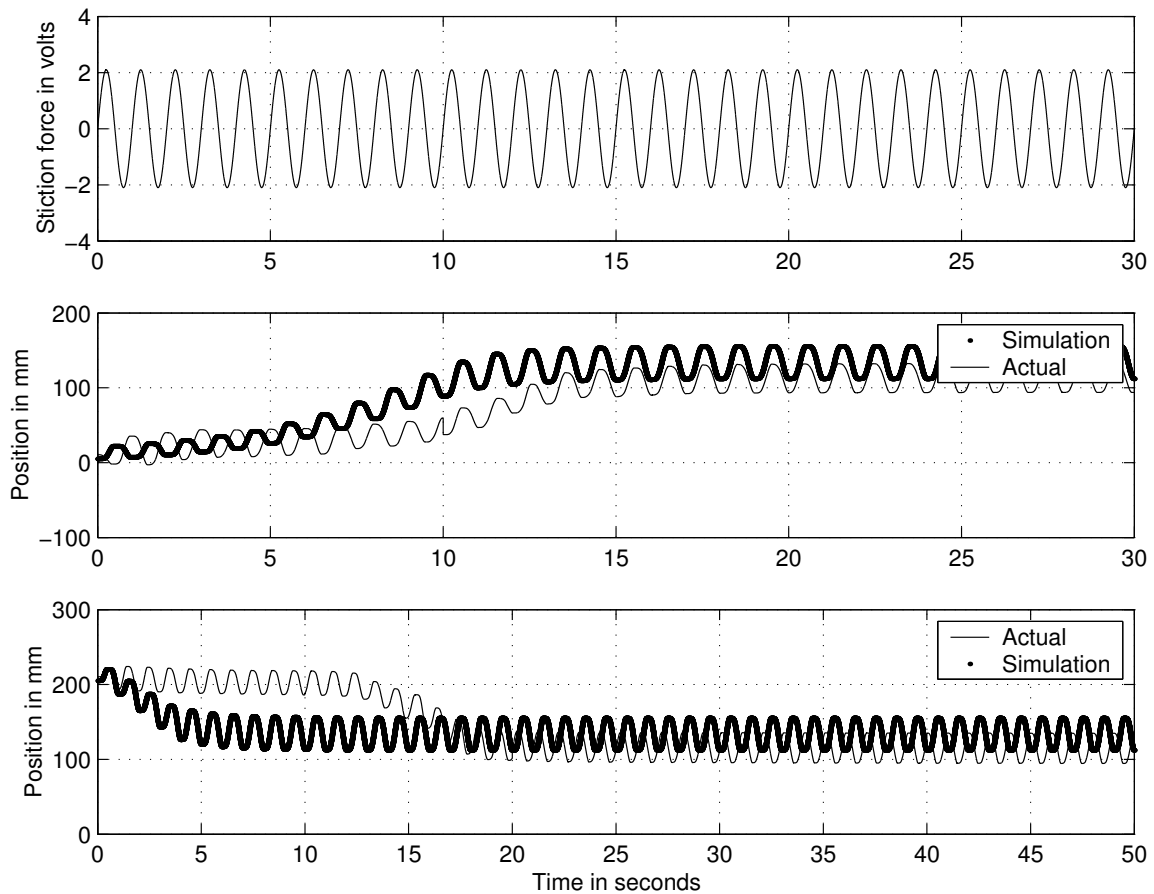


Fig. 27. Comparing the response of the above described model with the actual response

The experiment was designed to capture the stiction behavior for every 10mm. In order to capture stiction behavior, voltage of the input signal was increased from an initial value of 0.8V in steps on 0.1V until the slider moved by 10mm. Once the slider moved by 10mm or more, the input signal was reduced by a magnitude of 0.5V from the previously recorded value. The input signal was increased again in steps of 0.1V until the slider moved. The above process was repeated until the slider had traversed the entire range of travel in both the directions. Repeatability was ensured by conducting the experiment multiple times. The above experiment was automated. A similar kind of experiment has

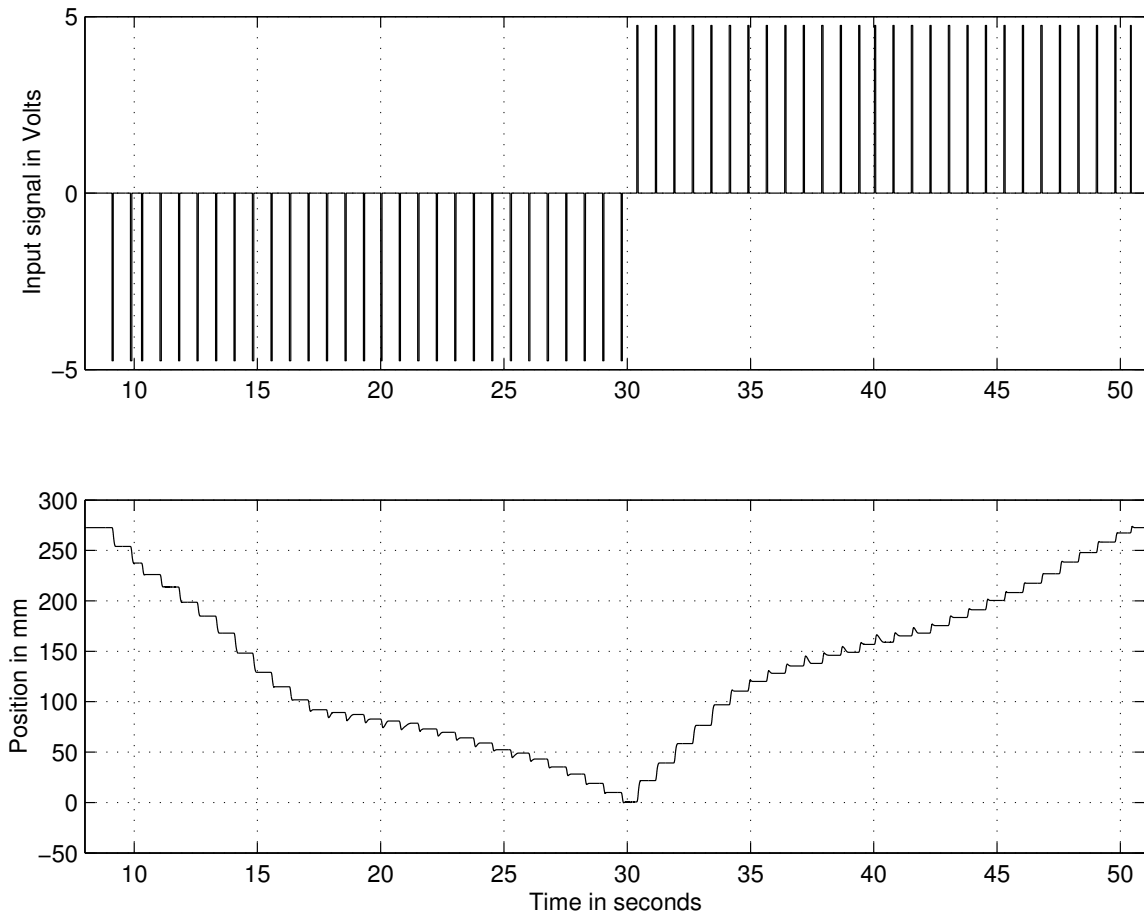


Fig. 28. The response of the slider to a constant signal

also been suggested in [18]

Figure 29 shows the data captured for the above described experiment for three trials. Table I details the voltage required to move the slider from rest against position data. A  $10^{th}$  order polynomial was used to fit the experimental data detailing the force required to overcome stiction along the length of the slider. Figure 30 shows stiction force profile as a function of the position of the slider and also the direction of motion. The region around the points where the two polynomials cross each other are stable regions, i.e the slider does not drift in these regions when excited by a zero mean periodic signal. The two stable points of interest occur at around 112mm and at around 215mm. The Coulomb friction profile is assumed to follow stiction profile. The magnitude of Coulomb friction force is considered to be less than the stiction force by a magnitude of 0.4V across the entire range.

## 1. Results

The simulation results of the above considered model are compared with the response of the system. The responses were compared for various combination of input signals and initial conditions. The input signals considered were zero mean sinusoidal and square waves. The various initial conditions considered were a) slider starting from 10mm b) slider starting from 205mm c) slider starting from 230mm and d) slider starting from 120mm. Figure 31 shows the comparison of the open loop response of the above described model and the system for a zero mean sinusoidal signal of amplitude 2.1V and frequency 1Hz. The initial condition of the slider is 10mm. Figure 32 shows the comparison of the open loop response of the above described model and the system for a zero mean sinusoidal signal of amplitude 2.1V and frequency 1Hz. The initial condition of the slider is 205mm. The nature of drift of the slider in open loop for a zero mean periodic signal is well predicted by the model. There is a mismatch on the amplitude scale between the model output and the actual response. This could be attributed to error in the estimation of the parametric



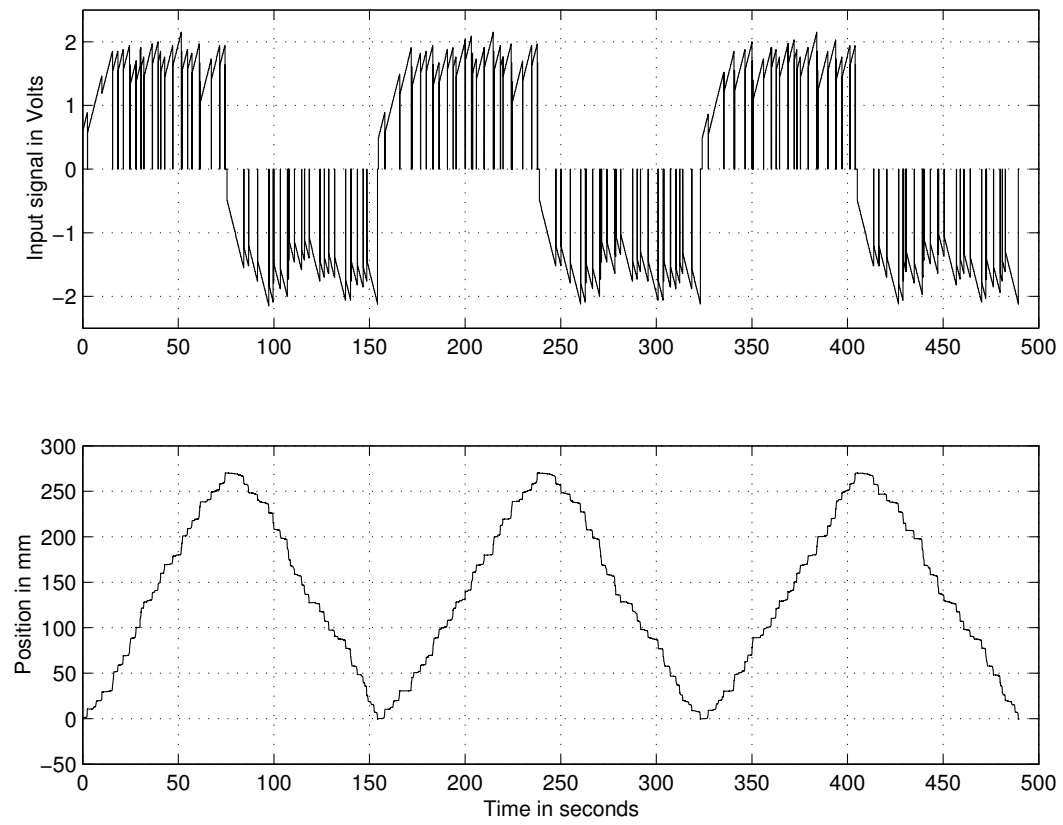


Fig. 29. Stiction profile along the length of the slider

Table I. Experimental Data

Moving left to right		Moving right to left	
Position(mm)	Input Signal(volts)	Position(mm)	Input Signal(volts)
0	0.83	0	2.05
10.5	0.86	8	1.96
12	1.04	15.5	1.82
20	1.4	18.5	1.64
31	1.85	26	1.58
40	1.6	36.5	1.73
45.5	1.37	46.5	1.82
52	1.76	57	1.79
59	1.79	68.5	1.73
70	1.88	76.5	2
82	1.6	87	1.91
89	1.61	97	1.7
92	1.62	98	1.55
100	1.64	107	1.55
101	1.82	115.5	1.67
108	1.79	126	1.7
110	1.85	128	1.4
121.5	1.7	136	1.28
128.5	1.61	146.5	1.31
130	1.82	157	1.58
131.5	1.97	168	1.4
140	2	179	1.4
141.5	2.03	188.5	1.67
150	1.76	197	1.94
161	1.67	207	1.82
169.5	1.85	217.5	1.76
180	2.09	227	2.03
191.5	1.83	237	2.06
202	1.87	239.5	1.63
212.5	1.7	247	1.73
220	1.91	257	1.46
228.5	1.6	267	1.46
234	1.33	270	1.43
241	1.64		
250	1.64		
252	1.88		
258	1.82		
270	1.78		

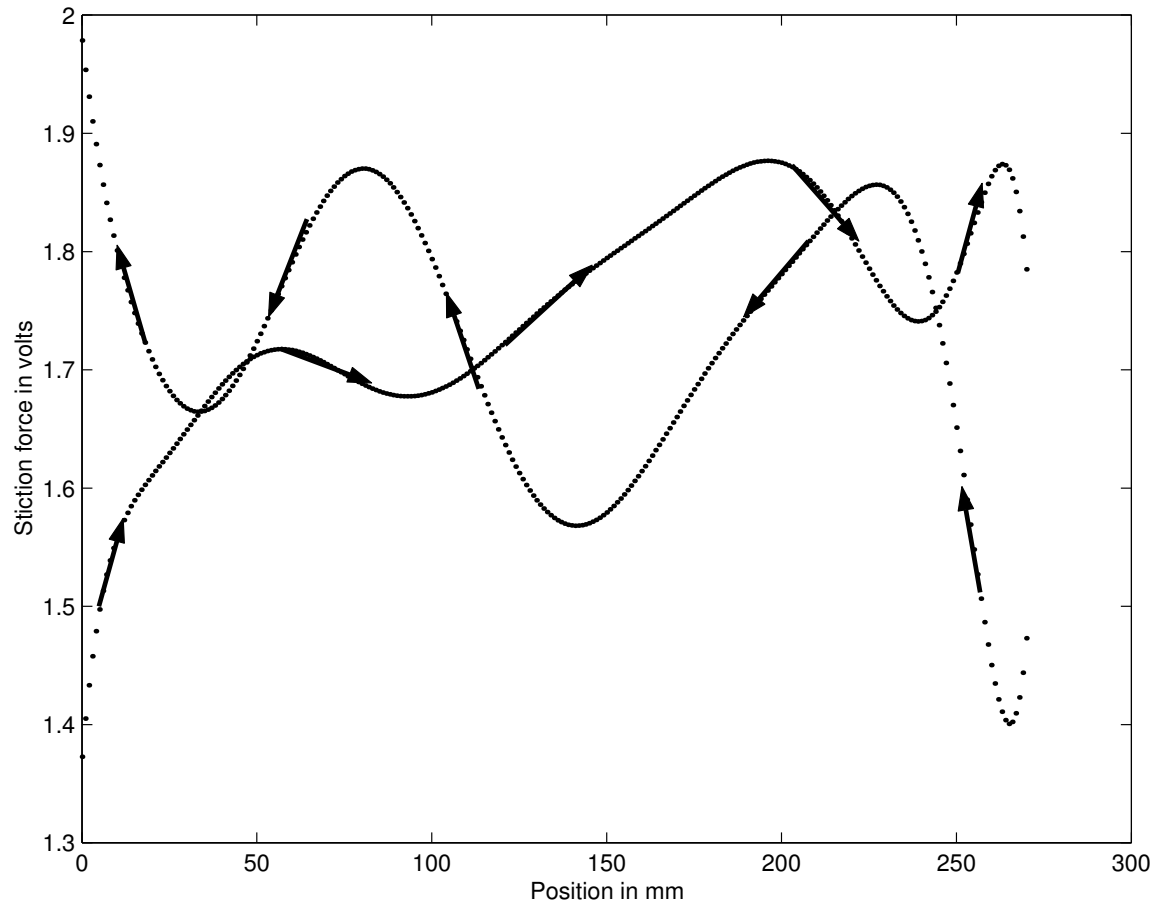


Fig. 30. Stiction profile

values of the model. Figure 33 shows the response of the model and the system for the above described sinusoidal input signal while starting at 115mm and 250mm. The reason the response to these initial conditions are shown together is because these are stable regions, i.e the slider does not drift in the open loop when excited by a zero mean periodic signal. Until now the model response has been compared to the actual system's response mainly for sinusoidal input signals. Sinusoidal signals capture the behavior of the system for a particular frequency. Square wave input signal contains all multiple harmonics of its fundamental frequency. Therefore, a square wave input would be helpful in evaluating the model response for a range of frequencies which are multiple harmonics of the fundamental frequency. Figure 34 shows the response of the model and the actual system when the input signal is a square wave of amplitude 3V and frequency 2Hz. The two initial conditions considered are 0mm and 215mm.

## 2. Friction Compensation

Friction compensation in its simplest form cancels the non-linearities due to friction. The various friction compensation techniques have been discussed in Chapter II. Model based friction compensation scheme has been considered for this thesis. This scheme is an example of feedback linearization technique. The friction observer estimates friction at any instant based on the position and velocity of the slider and the input signal to the system. Friction compensation in this case is also a tool to measure the validity of the friction model. In order to validate the friction model, the output of the system with friction compensation scheme is compared with the output of the system for an input signal of equal magnitude (but friction compensation being turned off). Also by comparing the system output when using friction compensation scheme with the output of an equivalent linear model in simulation. This would give an idea of how well the model is able to estimate and cancel friction. Furthermore, linear control system design techniques can be applied to

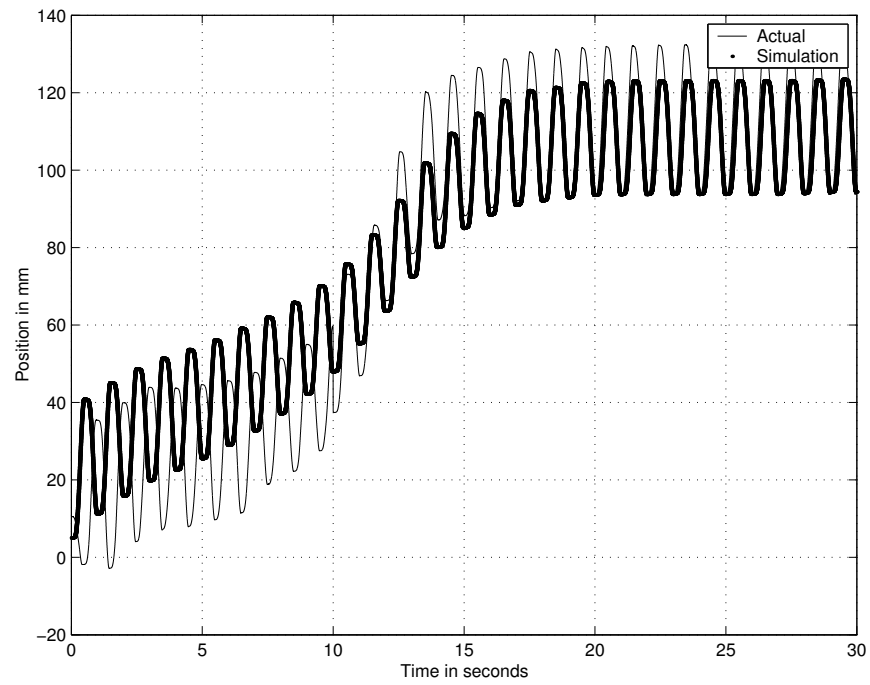


Fig. 31. Comparison of the open loop response of the model and the system, while starting at 10mm

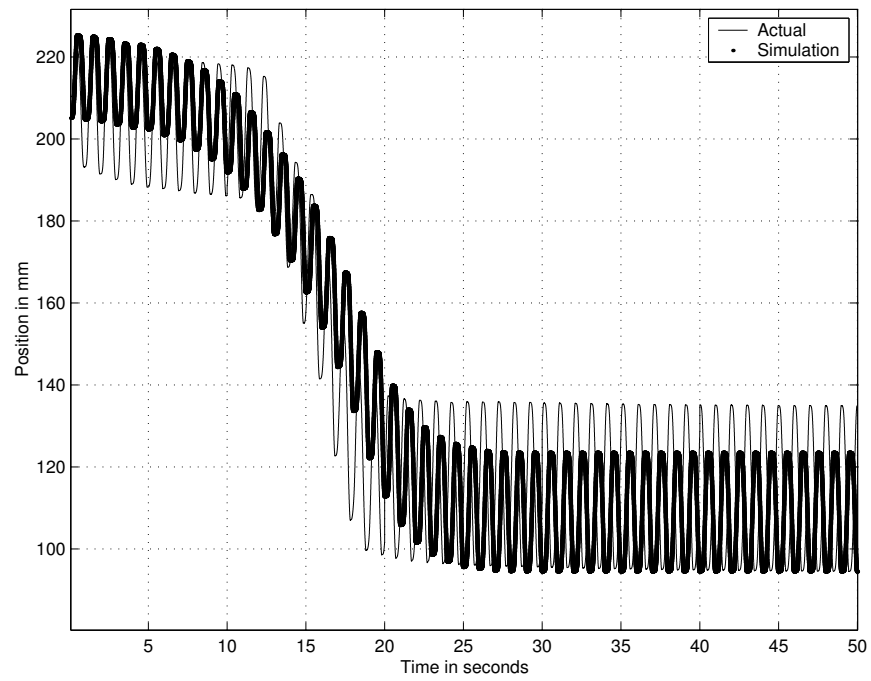


Fig. 32. Comparison of the open loop response of the model and the system, while starting at 205mm

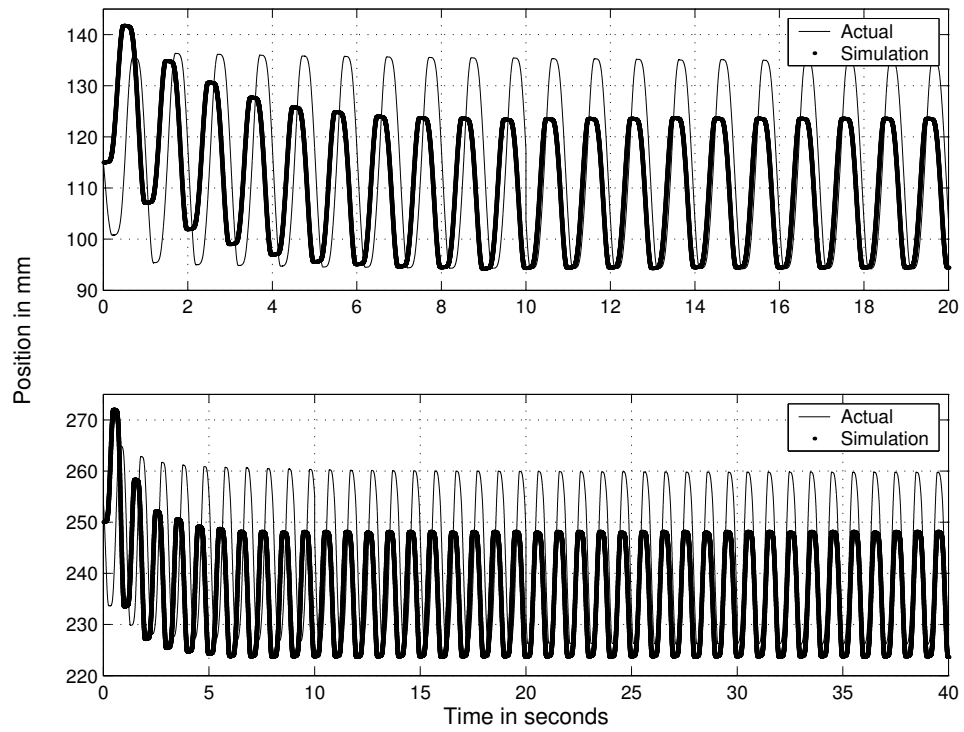


Fig. 33. Comparison of the open loop response of the model and the system, while starting at 115mm and 250mm

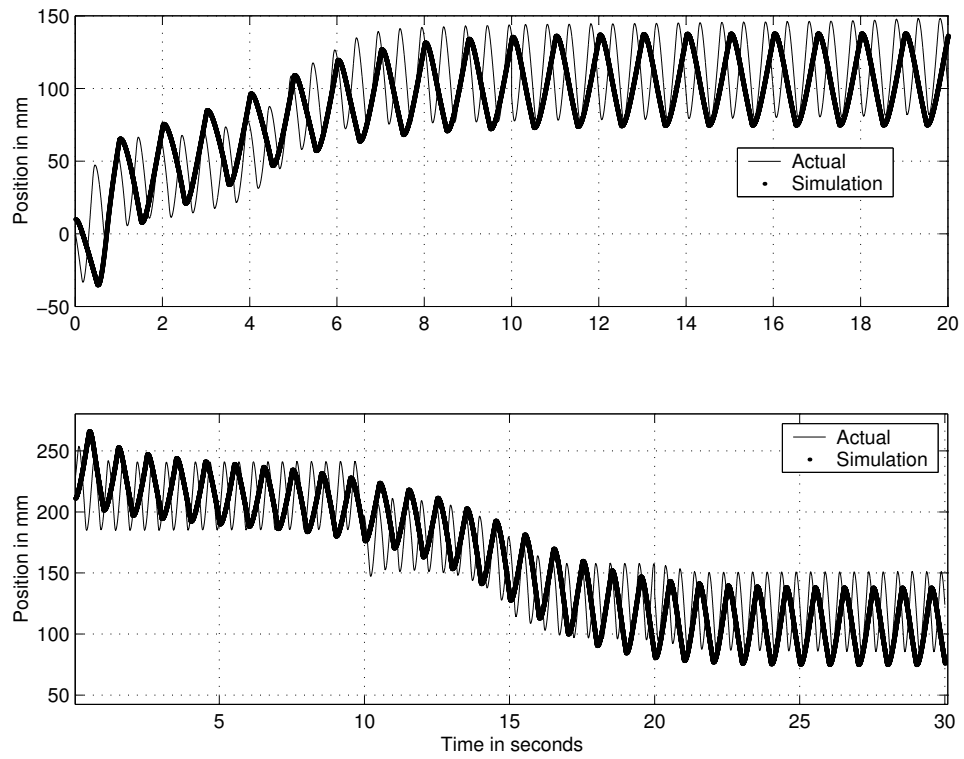


Fig. 34. Comparison of the open loop response of the model and the system for a zero mean square wave input



achieve various objectives.

Figure 35 shows the response of the slider when friction compensation scheme is active and without friction compensation. The open loop, zero mean, sinusoidal input signal of amplitude 0.75V and frequency 1Hz was used along with the friction compensation scheme. The effective signal to the system (with friction compensation) was of amplitude 2.25V and frequency 1Hz. The system was excited with a 2.25V (1Hz) signal without any friction compensation and same initial conditions. In this case, the slider drifts to the center while in the former case, where friction compensation was active, the slider does not drift. Thus, friction compensation scheme is able to cancel out the drift characteristics of the slider.

Figure 36 shows the comparison of the system (slider) output (with friction compensation) with the response of an equivalent linear system in simulation. The equivalent linear system in simulation is a second order system whose mass and coefficient of damping is equal to the mass and coefficient of damping of the slider as determined by the earlier mentioned experiment. The comparison gives an idea how well the friction compensation scheme is able to linearize the system. The solid black line at the center denotes the position of the slider when friction compensation was not active (the slider was stationary). The input signal was a zero mean sinusoidal signal of amplitude 0.75V and frequency 1Hz. The peak to peak amplitude of the system (with friction compensation) is around 54mm while the peak to peak amplitude of the linear system in simulation is 46mm. Thus, the identified friction model slightly over predicts the friction in the system. This is also evident when the system output in open loop is compared with the model output in simulation (Figures 31, 32, 33, 34). The amplitude of the output in simulation is less than the amplitude of the response of the system.

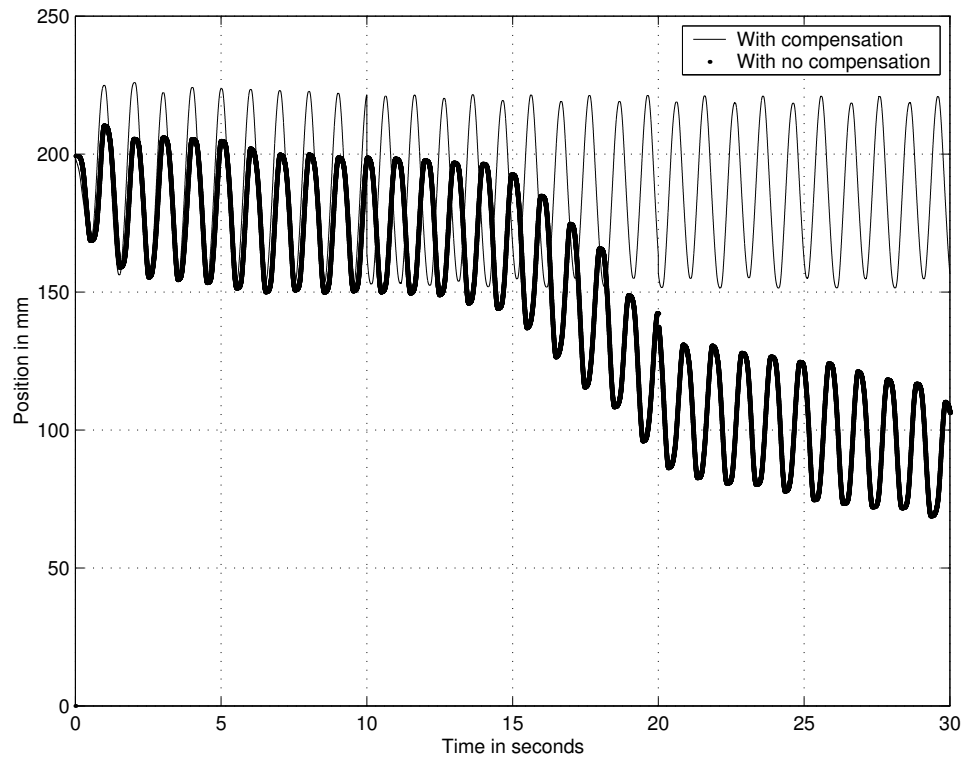


Fig. 35. Comparison of the response of the system with and without friction compensation

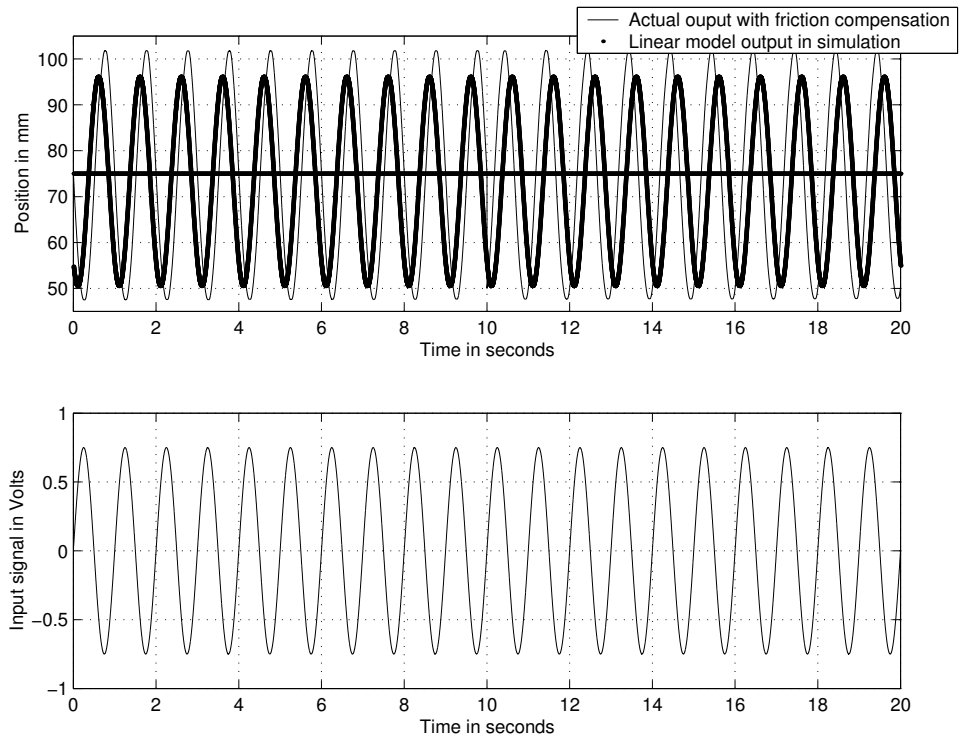


Fig. 36. Comparison of the response of the system with friction compensation and the response of an equivalent linear system

## CHAPTER V

### CONCLUSIONS AND FUTURE WORK

The main objectives of this thesis was to model the fine and the coarse stage of the dual stage actuator test bed in the lab and also implement simple friction compensation scheme for the coarse stage. The above mentioned objectives have been met. These objectives pertained to the specific set up in the laboratory. The more generic objective was to formulate a generic set of guidelines to identify friction in electromechanical systems. The major emphasis of this thesis was to identify friction in the coarse stage.

Friction in real time systems is usually a complex phenomena. Although static friction models are easy to implement in simulation, they do not necessarily capture the true behavior of friction in electromechanical systems. This fact has been reiterated in this thesis. Friction more than often is not just a function of velocity. The friction in the system considered is a function of position and velocity. Additionally, the friction is also dependent on the direction i.e, it is asymmetric with respect to the direction.

Based on the methodology followed and experiments conducted to identify friction for the coarse stage of the test bed, a generic guideline is being proposed to identify friction in electromechanical systems.

- 1) Initially, static friction models should be tried to model friction i.e, Coulomb friction model, Coulomb and stiction model, Coulomb, stiction and viscous friction model.
- 2) Using square waves of higher amplitudes, the effect of friction can be made negligible. The magnitude of the input signal depends on the system under consideration. Linear parameters of the model can be identified using the above scheme.
- 3) Capture the system response in open loop for various class of input signals. This gives an insight into the behavior of friction. For e.g, in this thesis the drift of the slider was observed for zero mean periodic signals.

4) Map stiction as a function of position by estimating force required to move the system, in small steps, from rest over the entire range of operation. The step size of motion is to be chosen based on the range of operation. Also, the magnitude of increase of force should be chosen such that it is able to capture stiction behavior as a function of position. If the magnitude is too large, stiction as a function of position would be too simple and if the magnitude is too small, stiction as a function of position would be too complex.

5) Coulomb friction can be assumed to follow the stiction profile.

In order to develop a better model of friction, Coulomb friction as a function of position can be determined independent of the stiction force. Coulomb friction as a function of position can be determined by ensuring the system moves at a constant velocity along the entire range of motion and by measuring the input signal required to maintain the constant velocity as a function of position [18] [19]. The above scheme could not be effectively in the laboratory due to noise in estimation of velocity (mainly due to numerical differentiation and partly sensor noise).

Future work could be estimation of Coulomb friction independent of the stiction force as described above. Various adaptive control schemes can be tried for friction compensation rather than just the model based compensation scheme. In the current compensation scheme no robustness is ensured. The compensation scheme was considered as a tool to evaluate the model. The initial objective when this thesis was started was to design a dual stage controller to ensure that the fine stage and the coarse stage work in conjunction.

## REFERENCES

- [1] M.Tomizuka, “Advanced control applications to servo systems for precision machines,” University of California at Berkeley, July 1997.
- [2] K.J.Aström, C.Canudas de Wit, and P.Lischinsky, “A new model for control of systems with friction,” *IEEE Transactions on Automatic Control*, vol. 40, no. 3, pp. 419–425, March 1995.
- [3] P.Dahl, “A solid friction model,” Technical Report 0158(3107-18)-1, The Aerospace Corporation, El Segundo, CA, 1968.
- [4] K.J. Aström, “Control of systems with friction,” Lund Institute of Technology, Lund, Sweden, August 1998.
- [5] D.Hernandez, S.S.Park, R.Horowitz, and A.K.Packard, “Dual-stage track-following servo design for hard disk drives,” in *Proceedings of the American Control Conference*, San Diego, CA, June 1999, pp. 4116–4121.
- [6] S.J.Schroeck and W.C.Messner, “On controller design for linear time-invariant dual-input single-output systems,” in *Proceedings of the American Control Conference*, San Diego, CA, June 1999, pp. 4122–4126.
- [7] F. Altpeter, “Friction modeling, identification and compensation,” Ph.D. dissertation, Ecole Polytechnique Federale de Lausanne, Lausanne, Switzerland, 1999.
- [8] H. Olson, K.J. Aström, C. Canudas de Wit, M. Gäfvert, and P. Lischinsky, “Friction models and friction compensation,” *European Journal of Control*, vol. 4, pp. 176–195, December 1998.

- [9] D.Karnopp, “Computer simulation of slip-stick friction in mechanical dynamic systems,” *Journal of Dynamic Systems, Measurement, and Control*, vol. 107, no. 1, pp. 100–103, 1985.
- [10] B. Armstrong-Hélouvry, P. Dupont, and C.Canudas de Wit, “A survey of models, analysis tools and compensation methods for the control of machines with friction,” *Automatica*, vol. 30, no. 7, pp. 1083–1138, 1994.
- [11] R.H.A. Hensen, “Controlled mechanical systems with friction,” Ph.D. dissertation, Technische Universiteit Eindhoven, Eindhoven, The Netherlands, 2002.
- [12] N. van Seters, “Compensation of friction in the flight simulator stick using an adaptive friction compensator,” M.S. thesis, University of Twente, The Netherlands, June 2001.
- [13] S.Colombi, “Comparison of different control strategies and friction compensation algorithms in position and speed controls,” in *IFAC Workshop on Motion Control*, Munich, Germany, October 1995, pp. 173–180.
- [14] L. Iannelli, “Dither for smoothing relay feedback systems: an averaging approach,” Ph.D. dissertation, University of Naples Federico II, Napoli, Italy, 2002.
- [15] D. Stajić, N. Perić, and J. Deur, “Friction compensation methods in position and speed control systems,” in *Proceedings of IEEE International Symposium on Industrial Electronics*, July 1999, pp. 1261–1266.
- [16] J.E. Slotine and W. Li, *Applied Nonlinear Control (1st ed.)*, Englewood Cliffs, NJ:Prentice Hall, 1991.
- [17] Y.Chen, P.Huang, and J.Yen, “Frequency-domain identification algorithms for servo systems with friction,” *IEEE Transactions on Control Systems Technology*, vol. 10,

no. 5, pp. 654–665, September 2002.

- [18] E.G. Papadopoulos and G.C. Chasparis, “An analysis and model-based control of servomechanisms with friction,” in *Proceedings of International Conference on Intelligent Robots and Systems*, July 2002, pp. 2109–2114.
- [19] B. Armstrong-Hélouvy, *Control of Machines with Friction*, Norwell, MA: Kluwer Academic Publishers, 1991.



## VITA

Satish Thimmalapura received his Bachelor of Engineering degree in mechanical engineering from Bangalore University, Bangalore, India in 1999. Since 2001 he has been in the Master of Science Program in mechanical engineering, Texas A&M University, College Station.

## Permanent Address:

Satish Thimmalapura  
No:65, 6<sup>th</sup> Main Road  
C.H.B.S 1<sup>st</sup> Layout, Vijaynagar  
Bangalore, INDIA - 560040  
Phone: (979)676-1661  
Email: vtsatish@hotmail.com